USGS
science for a changing world

Prepared in cooperation with the National Oceanic and Atmospheric Administration, National Marine Fisheries Service

Using the Stream Salmonid Simulator (S3) to Assess Juvenile Chinook Salmon (*Oncorhynchus tshawytscha*) Production Under Historical and Proposed Action Flows in the Klamath River, California

Open-File Report 2019–1099

U.S. Department of the Interior
U.S. Geological Survey

Cover: Klamath River near Happy Camp, California, looking downstream.
Photograph by Christian Romberger, U.S. Fish and Wildlife Service, October 24, 2018.

Using the Stream Salmonid Simulator (S3) to Assess Juvenile Chinook Salmon (*Oncorhynchus tshawytscha*) Production Under Historical and Proposed Action Flows in the Klamath River, California

By John M. Plumb, Russell W. Perry, Nicholas A. Som, Julie Alexander, and Nicholas J. Hetrick

Prepared in cooperation with the National Oceanic and Atmospheric Administration, National Marine Fisheries Service

Open-File Report 2019–1099

U.S. Department of the Interior
U.S. Geological Survey

U.S. Department of the Interior
DAVID BERNHARDT, Secretary

U.S. Geological Survey
James F. Reilly II, Director

U.S. Geological Survey, Reston, Virginia: 2019

Suggested citation:
Plumb, J.M., Perry, R.W., Som, N.A., Alexander, J., and Hetrick, N.J., 2019, Using the stream salmonid simulator (S3) to assess juvenile Chinook salmon (*Oncorhynchus tshawytscha)* production under historical and proposed action flows in the Klamath River, California: U.S. Geological Survey Open-File Report 2019-1099, 43 p., https://doi.org/10.3133/ofr20191099.

ISSN 2331-1258 (online)

Contents

Figures

Tables

Conversion Factors

U.S. customary units to International System of Units

Multiply	By	To obtain
	Length	
inch (in.)	2.54	centimeter (cm)
inch (in.)	25.4	millimeter (mm)
mile (mi)	1.609	kilometer (km)
	Area	
square mile (mi^2)	259.0	hectare (ha)
square mile (mi^2)	2.590	square kilometer (km^2)
	Flow rate	
cubic foot per second (ft^3/s)	0.02832	cubic meter per second (m^3/s)

International System of Units to U.S. customary units

Multiply	By	To obtain
	Length	
kilometer (km)	0.6214	mile (mi)
	Area	
square kilometer (km^2)	0.3861	square mile (mi^2)
	Volume	
L (liter)	0.2642	gallon (gal)

Temperature in degrees Celsius (°C) may be converted to degrees Fahrenheit (°F) as follows:

$$°F=(1.8×°C)+32$$

Abbreviations

DNA	deoxyribonucleic acid
ESA	Endangered Species Act
EWA	environmental water account
FWS	U.S. Fish and Wildlife Service
HI	Historical (scenario)
KBPM	Klamath Basin Planning Model
NMFS	National Marine Fisheries Service
PA	Proposed Action (scenario)
POI	prevalence of infection
Reclamation	Bureau of Reclamation
rkm	river kilometer
S3	Stream Salmon Simulator
USGS	U.S. Geological Survey
WUA	weighted usable habitat area

Using the Stream Salmonid Simulator (S3) to Assess Juvenile Chinook Salmon (*Oncorhynchus tshawytscha*) Production Under Historical and Proposed Action Flows in the Klamath River, California

By John M. Plumb[1], Russell W. Perry[1], Nicholas A. Som[2], Julie Alexander[3], and Nicholas J. Hetrick[2]

Executive Summary

The production of Klamath River fall Chinook salmon (*Oncorhynchus tshawytscha*) in northern California and southern Oregon is thought to be limited by poor survival during freshwater juvenile life stages, in part a result of *Ceratonova shasta*—a highly infectious disease that can lead to high fish mortality. Higher flushing river flows are thought to affect the concentration of *C. shasta* spores, and in turn, juvenile salmon infection and mortality. The Stream Salmonid Simulator (S3) model was built to simulate the spatiotemporal dynamics of the growth, movement, and survival of juvenile salmon from spawning through migration to the Pacific Ocean in response to river flow, habitat availability, water temperature, and *C. shasta* spore concentrations. The S3 model has been calibrated to juvenile fall Chinook salmon abundances at a trap site within the Klamath River, and was specifically designed to provide objective predictions of juvenile salmon abundance and survival in relation to proposed flow management alternatives and resulting fish infection and mortality by *C. shasta*. Infection by *C. shasta* in the Klamath River is location specific, occurring in a "disease zone" with high spore concentrations. The spatial extent of this disease zone (from river kilometer 289.6 to 212.9) has been incorporated in the S3 model for the Klamath River, enabling the assessment of disease effects on fish at specific spatial locations such as the trap sampling sites, and for fish that were or were not exposed to the disease zone as they emigrate the Klamath River to the Pacific Ocean.

Given the information gained from field observations on spore concentrations in relation to river flow, deliberations by resource managers resulted in the incorporation of springtime flushing flows in a Proposed Action (PA) scenario developed in part to lower spore concentrations within the disease zone. A Historical (HI) scenario based on the observed flows, temperatures, and spore concentrations from 2004 to 2016 was used to compare and contrast the potential benefits to juvenile salmon from PA flows in relation to the HI conditions.

---

[1]U.S. Geological Survey.
[2]U.S. Fish and Wildlife Service.
[3]Oregon State University.

S3 model simulations of the HI and PA scenarios showed that salmon populations exposed to the disease zone had lower rates of *C. shasta* infection and lower mortality and had higher abundance at ocean entry under the PA scenario compared to the HI scenario, suggesting that the number of returning adults would have also been higher had PA flows been implemented during the same years. In-river water temperatures were very similar between the scenarios, and so contributed little to *C. shasta* infection rates between the scenarios. Thus, the premise that higher flushing flows will lead to lower rates of infection and mortality of juvenile Chinook salmon by *C. shasta* is supported by S3 model simulations. Using two locations of the Klamath River as benchmarks from which to assess the simulated outcomes (the Kinsman Creek trap site and the Pacific Ocean), the S3 model indicated greater abundances (22,257 more juveniles; a difference of -1 to 66 percent), lower prevalence of infection (5 compared to 11 percent), higher survival to the ocean (3.8 compared to 3.3 percent), and likely higher annual adult equivalent returns (mean = 978 more adult salmon; range = -64 to 3,452) under the PA compared to the HI scenario. For fish populations upriver of the disease zone in years when spore concentrations were high, our findings support the conclusion that the flows and decreased *C. shasta* spore concentrations under the PA scenario would lead to lower infection and in-river mortality for juvenile salmon relative to the HI conditions.

Introduction

Background

Federal resource agencies responsible for managing Endangered Species Act (ESA; 16 U.S.C. 1531 et seq.) listed fisheries are charged with using the best available science to analyze the effects of water management on listed salmon in the Klamath River, northern California and southern Oregon. For the Klamath River, Bureau of Reclamation (Reclamation) consults with the National Marine Fisheries Service (NMFS) on the effects of the Reclamation Klamath Project on listed Southern Resident Killer Whales (*Orcinus orca*), which are reliant on Chinook salmon
(*Oncorhynchus tshawytscha*) as a food resource. On December 21, 2018, Reclamation formally requested an ESA section 7 consultation with NMFS and U.S. Fish and Wildlife Service (FWS) on a Proposed Action that incorporates new science in a proposed flow regime for the Klamath River. NMFS has requested the technical support of the U.S. Geological Survey (USGS) and FWS to analyze the Proposed Action of Reclamation on Chinook salmon populations.

USGS and the FWS developed the Stream Salmonid Simulator (S3) to help Klamath Basin resource managers evaluate the effect of management alternatives on juvenile salmonid populations. S3 is a deterministic stage-structured population model that tracks daily growth, movement, and survival of juvenile salmon (Perry and others, 2018). A key theme of the model is that river flow affects habitat availability and capacity, which in turn controls density-dependent population dynamics. The S3 model for the Klamath River is unique in that it incorporates a model of infection and mortality of juvenile salmon by *Ceratonova shasta* while incorporating survival and movement parameters that are calibrated to juvenile abundance estimates collected by an annual monitoring program (Perry and others, 2019). Different tributary-specific populations of Chinook and Coho salmon (*O. kisutch*) entering the Klamath River have different exposure to the *C. shasta* owing to the timing of main-stem entry to the Klamath River and location of each tributary mouth relative to the location of the *C. shasta* infectious zone (Bartholomew and others, 2015; fig. 1). Understanding how changes in Klamath River flows, the effect of flow on *C. shasta* dynamics, and the consequent effect of these factors

on tributary-specific juvenile fish production is critical for managing regulated flows to recover and maintain salmon populations. Toward this end, the S3 model has been uniquely designed to help users understand how alternative management actions may affect disease, and in turn, dynamics of tributary source populations of juvenile salmon in the Klamath River.

Purpose and Scope

This report summarizes the simulated population dynamics of Klamath River juvenile Chinook salmon by running the S3 model under two scenarios: (1) Historical conditions (hereinafter, HI), and (2) the Reclamation Proposed Action (hereinafter, PA). The HI scenario simulates population dynamics under the observed biological and physical conditions that include the following:

- Female spawner abundance,
- The abundance of juvenile salmon entering the Klamath River from tributaries and main-stem spawners,
- Daily *C. shasta* spore concentration in the infectious zone,
- Historical dam operations and tributary accretions, and
- Simulated water temperatures predicted using observed river flows and meteorological conditions.

The PA scenario includes modifications of the HI scenario in four key ways: (1) discharge released from Iron Gate Dam, (2) predictions of habitat availability, (3) predictions of *C. shasta* spore concentrations, and (4) simulated water temperatures in response to PA flows. All other model inputs were kept constant between scenarios such that the differences between scenarios in physical (flows, habitat, and water temperatures) and biological (spore concentrations) conditions were the primary drivers of differences in the population response between scenarios. Thus, this report summarizes S3 model outputs in terms of juvenile fish production, survival, and prevalence of infection and eventual mortality by *C. shasta* under the HI and PA scenarios.

Study Site

The Klamath River Basin covers more than 15,000 mi^2 and is divided into two subbasins (upper and lower) at Iron Gate Dam (river kilometer [rkm] 312; fig. 1). Although not a focus for this report, the upper basin area includes parts of Klamath, Lake, and Jackson Counties in Oregon, and Siskiyou and Modoc Counties in California. The lower basin area includes parts of the Siskiyou, Modoc, Trinity, Humboldt, and Del Norte Counties in California. The Klamath River Basin is unlike most watersheds, with a unique geomorphology opposite of that present in most other drainage basins and has been called “a river upside down” by the National Geographic Society (Weddell, 2000; Rymer, 2008). Much of the upper Oregon section of the basin is flat and open, in comparison to the narrow canyons and mountainous terrain present in the lower California section of the basin.

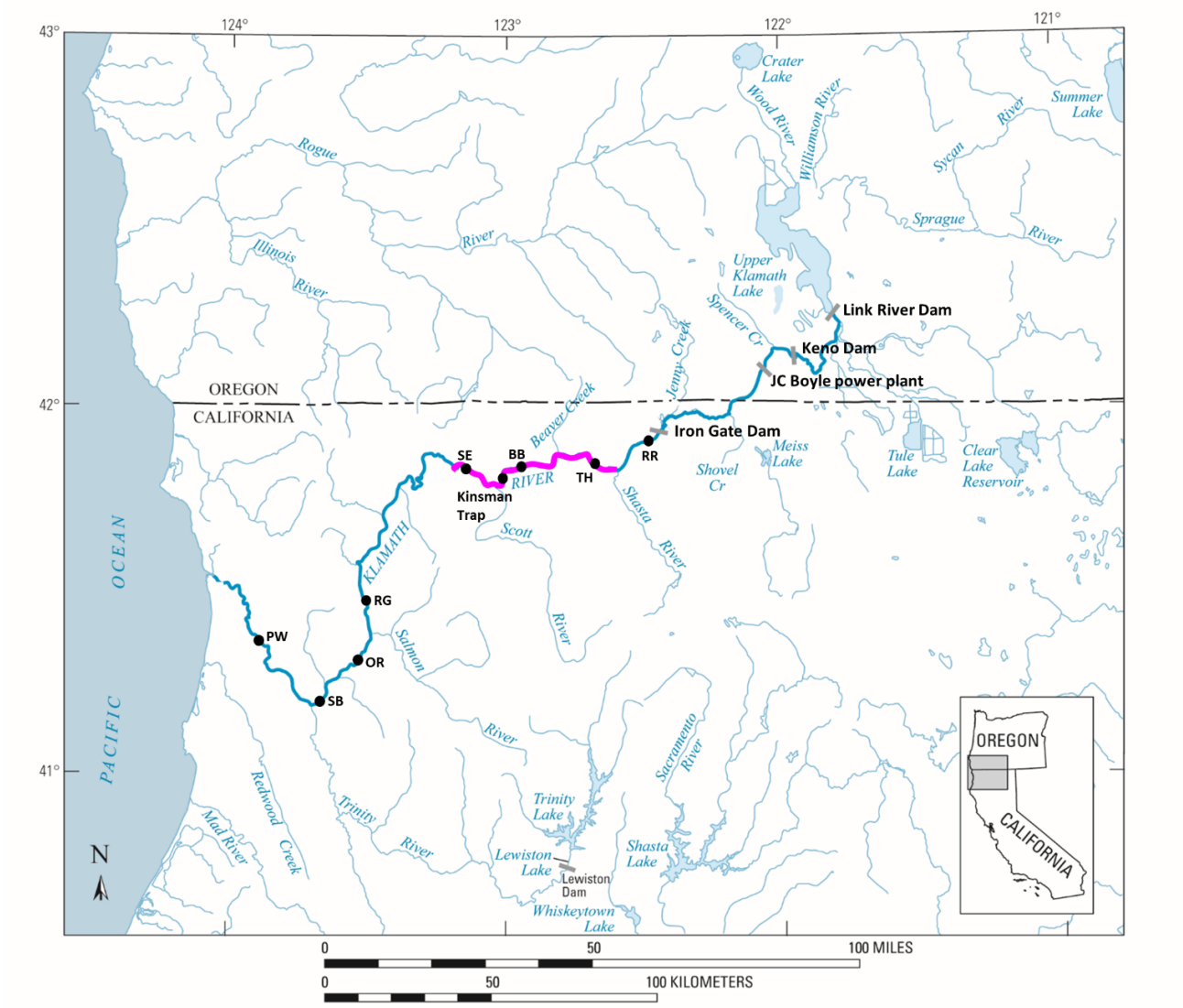

Figure 1. Map showing locations of major tributaries, dams, the Kinsman fish trap just upstream of the confluence with the Scott River, the *Ceratonova shasta* disease zone (thick pink line), and locations of two-dimensional hydrodynamic models used for Chinook salmon habitat modeling (RR, R Ranch; TH, Trees of Heaven; BB, Brown Bear; SE, Seiad; RG, Rogers; OR, Orleans; SB, Saints Bar; PW, Pecwan), on the Klamath River, Oregon and California.

The upper Klamath River Basin lies in the rain shadow of the Cascade Range on the west, the Deschutes River Basin on the north, the Great Basin on the east, and the Pit River Basin on the south. The upper basin consists mostly of agriculture and rangeland with areas of pine forest and semiarid high-desert plateaus, and is characterized by low-relief, volcanic geology with an average annual precipitation of 34.89 in. (California Rivers Assessment, 2011). The Klamath River is impounded by six dams, and four large hydroelectric dams are being considered for removal in 2021 (U.S. Department of Interior, 2013). The farthest upstream is Keno Dam (rkm 378.2) and the farthest downstream facility is Iron Gate Dam (rkm 312; fig. 1), which blocks the migration of anadromous salmon to the upper Klamath River Basin. The lower Klamath River Basin is mostly forested except for areas of agriculture and rangeland in the

drainages of the Scott and Shasta Rivers. The lower Klamath River Basin is dominated by a steep, rugged, complex terrain (also known as the Klamath Mountains), and alluvial reaches. Average annual precipitation for the lower basin is 79.62 in. (California Rivers Assessment, 2011).

In this report, we focus on the section of the Klamath River between Iron Gate Dam and the ocean. This section of the Klamath River is critical habitat used by several anadromous salmonids, including spring and fall run Chinook salmon, Coho Salmon, and Steelhead Trout (*Oncorhynchus mykiss*). Additionally, several large tributaries contribute water and juvenile Chinook salmon to the main-stem Klamath River. These tributaries are:

- Bogus Creek (rkm 311.6),
- Shasta River (rkm 289.6),
- Scott River (rkm 232.8),
- Salmon River (rkm 107.5), and
- Trinity River (rkm 70.6).

Methods

We apply herein the S3 simulation model to juvenile Chinook salmon in the Klamath River in response to flows, water temperatures, and spore concentrations modeled under the HI and PA scenarios. To run these scenarios, we use the version of the S3 model built specifically for Klamath River Chinook salmon populations. The key features of this model relevant to Klamath Project operations include (1) a *C. shasta* disease submodel, and (2) density-dependent dynamics that are influenced by the effect of flow on suitable habitat area. Specifically, Perry and others (in review) noted that density-dependent movement fit observed abundance data better than a model with density-dependent survival. The disease submodel simulates (1) the probability of becoming infected with *C. shasta* and eventually dying from ceratomyxosis, and (2) the time to death of infected individuals. Both infection and time to death are simulated as functions of time since initial exposure to *C. shasta*, water temperature, and spore concentration and duration of exposure (dose). In this report, we briefly describe the model inputs and outputs as necessary to understand the structure of each scenario and the basic drivers of population dynamics under each scenario. We encourage readers to consult Perry and others (2019) for a complete description of the Klamath River S3 model, and Perry and others (2018), which details the mathematical structure of the S3 model.

Stream Salmonid Simulator Model Inputs

Habitat Template and Physical Inputs

The spatial domain of the S3 model is defined by a one-dimensional representation of discrete habitat units. In total, the Klamath S3 model has 2,635 habitat units positioned between Keno Dam and the ocean. The 312-km section of river between Iron Gate Dam and the ocean modeled here consists of 1,706 discrete habitat units that were classified as specific mesohabitat types such as riffles, runs, pools, and braided channels (Perry and others, 2019). For more detailed information on how meso-habitat units were determined for sections of the Klamath River in both impounded and unimpounded sections of the Klamath River, readers are encouraged to see Hardy and Shaw (2011).

The S3 model requires two physical inputs, water temperature and stream flow, that drive population dynamics either directly or indirectly. Daily water temperature dictates biological rates of development such as maturation of eggs in the gravel, growth of juveniles after emergence, and disease susceptibility and mortality owing to *C. shasta*. River discharge affects available habitat for juveniles, and in turn, density-dependent dynamics (Perry and others, 2019). Additionally, river discharge affects habitat suitability of the polychaete worm *Manayunkia speciosa*, the intermediate host for *C. shasta*, which in turn affects the concentration of spores released by the polychaete.

Inputs for the S3 model also require relationships between discharge and the amount of suitable habitat provided by each habitat unit in the model domain. The available habitat area for each unit was quantified using an extrapolation procedure that scaled weighted usable habitat area (WUA) curves constructed from two-dimensional hydrodynamic models for eight distinct geomorphic reaches of the Klamath River (see fig. 1) to each habitat unit of the S3 model domain (Perry and others, 2019).

Flow, Temperature, and Weighted Usable Habitat Area Inputs for Historical and Proposed Action Scenarios

Under its Proposed Action, Reclamation proposes to manage the complex network of water storage and conveyance features in the Klamath Basin to operate the Klamath Project to meet contractual water delivery obligations, remain compliant with State and Federal laws, and maintain Klamath River hydrologic conditions and Upper Klamath Lake elevations to avoid jeopardizing the continued existence of listed species (National Marine Fisheries Service, 2019). The PA covers a 5-year period extending from 2019 to 2024 and includes water-management prescriptions that arose from a process of repeated applications of the Klamath Basin Planning Model (KBPM). The KBPM simulates Klamath Project operations over a hydrologic period of record that includes water years (from October 1 to September 30 the following year) from 1981 to 2016. Interested readers can find a more detailed description of the KBPM in appendix 4 of the Bureau of Reclamation addendum to the Klamath Project Operations Final Biological Assessment (Bureau of Reclamation, 2019).

This report focuses on simulating the potential effects of water management, as described in the PA, on the population dynamics of Chinook salmon in the Klamath River. Hence, we focus herein on the aspects of the PA that directly relate to water-management prescriptions regarding discharge levels from Iron Gate Dam, and readers interested in other aspects of the PA are encouraged to consult the description of the PA contained in NMFS Biological Opinion (National Marine Fisheries Service, 2019). In each annual simulation of the PA, hydrologic conditions and Upper Klamath Lake inflow forecasts are assessed, and total water supply is allocated for Klamath Project delivery, storage in Upper Klamath Lake, or release to the Klamath River through an environmental water account (EWA).

For the period March 1–September 30, the EWA volume is distributed to the Klamath River on a daily basis with an overall goal of minimizing disease risk and providing habitats required for rearing and migration of salmonids (National Marine Fisheries Service, 2019). Under the PA, disease mitigation flows are intended to disrupt the complex life cycle of *C. shasta* by adversely affecting the abundance of polychaete worms and their habitats by releasing surface flushing flows from Iron Gate Dam that meet or exceed 6,030 ft^3/s for at least 72 consecutive hours (Som and others, 2016). Distribution of the EWA targeted to address habitat needs is allocated through an approach aimed to mimic some characteristics of a natural flow regime (National Marine Fisheries Service, 2019). This is accomplished by balancing remaining

EWA volume with the number of days remaining in the management period and specified minimum flows that change each month, and then scaling river flows to observed inflows into Upper Klamath Lake (National Marine Fisheries Service, 2019). The actual "formulaic approach" that is applied in order to set flow targets on each day is complex, and interested readers are encouraged to consult details in the NMFS Biological Opinion (National Marine Fisheries Service, 2019).

Although the formulaic approach in the Reclamation PA differs somewhat from that implemented under previous management regimes, the overall tenet remains: an indicator-based flow pattern aimed to mimic elements of a natural flow regime. The management element differing from prior PAs as it relates to river discharges is the implementation of environmental flow releases in the form of surface flushing and deep flushing flows. Surface flushing flows are forced to occur in most years whereas deep flushing flows are intended to occur when hydrology and public safety concerns allow. Evaluating the effectiveness of the PA in the context of disease infection and mortality rates required development of a method to alter the observed water concentrations of *C. shasta* spores.

To run the HI and PA simulations, the S3 model required flow and temperature inputs as a time series of daily mean water temperature (in degrees Celsius) and daily mean discharge (in cubic foot per second) for discrete reaches of the modeled spatial extent. For the HI scenario, daily river flows were constructed from Iron Gate Dam releases and gaged tributary inputs, and accretions from ungaged tributaries were estimated by apportioning unassigned gaged flows of the Klamath River in proportion to the watershed area of ungaged tributaries (see Perry and others, 2019). For the PA, Reclamation provided a daily time series of Iron Gate flows for the period of record (1981–2016). Downstream river flows were then constructed using historically observed tributary flows and ungaged accretions distributed proportional to watershed area, as done for the HI scenario.

River flows for each scenario were then used as inputs for water temperature and WUA models. For WUA, the time series of river flows for each scenario were used to develop a time series of available habitat using methods described in Perry and others (in review). For water temperature, we input the daily flows for each scenario into the RBM10 stream temperature model (Perry and others, 2011) using the historic meteorology for example, air temperature, solar radiation) for the period of record. For inputs into S3, simulated water temperatures were output at 20 locations. Daily flow and temperature were assumed constant between output locations and then mapped to each habitat unit in S3 to create a daily time series for each habitat unit.

Biological Inputs

The S3 model relies on the three primary forms of biological inputs to simulate population dynamics: (1) female spawners, (2) juvenile fish entering from tributaries and hatchery releases, and (3) a daily time series of spore concentrations. For spawners and juveniles, inputs for S3 were based on annual abundance estimates from monitoring programs, which were held constant for both scenarios. For the HI scenario, we constructed a daily time series of spore concentrations using a data set of weekly measured spore concentrations collected since 2005 (see Perry and others, 2019). The HI time series of spore concentrations was modified for the PA scenario according to the hypothesized effect of the Proposed Action flows on polychaete habitat and abundance.

Female Spawners

To develop inputs for the number of female spawners, spawner survey data were summarized as a weekly time-series of redd counts or female abundance estimates by survey reach (Gough and Som, 2015). To form model inputs, weekly reach-level redd counts were distributed uniformly across days within each week and then assigned to each habitat unit in proportion to available spawning area (Perry and others, 2019). Surveys were not conducted downstream of rkm 178 owing to low use of the lower Klamath River for spawning. Therefore, we assumed that no spawning occurred downstream of rkm 178.

Juveniles from Tributaries and Hatcheries

In addition to natural production within the main-stem Klamath River, seven other source populations contribute juveniles to the section of the Klamath River located between Iron Gate Dam and the Pacific Ocean:

1. Iron Gate Hatchery,
2. Bogus Creek,
3. Shasta River,
4. Scott River,
5. Salmon River,
6. Trinity River, and
7. Trinity River Hatchery.

Abundance estimates by release date were obtained from Iron Gate Hatchery. Weekly abundance estimates of juveniles entering the Klamath River were obtained from agencies that operated juvenile fish traps on tributary streams. The FWS provided abundance estimates for Bogus Creek and the Trinity River (Gough and others, 2015). California Department of Fish and Wildlife provided abundance estimates for the Shasta and Scott Rivers (for example, see Daniels and others, 2011), and Karuk Native American Tribe provided estimates of adult escapement for the Salmon River. For constructing model inputs, all weekly abundance estimates were distributed uniformly across days within each reach.

For the Salmon River, juvenile production was estimated based on a stock-recruitment relationship that estimated capacity as a function of watershed area and productivity as a function of the median outmigration date of juveniles (Hendrix and others, 2011). For example, the number of recruits R_{y+1} from a given brood year y of spawners S_y may be expressed as:

$$R_{y+1} = \alpha \cdot S_y \cdot e^{-(\frac{1}{S_{\max}})\cdot S_y}$$
$$S_{\max} = e^{2.11} \cdot WA^{0.965} \quad , \qquad (1)$$

where baseline productivity a is 78.8 recruits per spawner, $S_{\max}$ is 12,260 spawners in a watershed area (WA) for the Salmon River of 1,937 square kilometers.

Ceratonova shasta Spore Concentrations

To simulate infection and mortality of juvenile salmon caused by *C. shasta*, S3 requires inputs of daily *C. shasta* spore concentrations. Therefore, we developed a daily time series of spore concentrations using measurements of the quantity of *C. shasta* deoxyribonucleic acid (DNA) in water samples collected weekly in the Klamath River near Beaver Creek (rkm 263.5) from 2005 to 2018. For the HI scenario, water samples were analyzed by the Aquatic Animal Health Laboratory at Oregon State University using quantitative polymerase chain reaction techniques (Hallett and Bartholomew, 2006). DNA quantity was measured as cycle threshold values and converted to spore concentration (in spores per liter [spores/L]). See Perry and others (in review) for further details on methods used to develop a daily time series of spore concentrations.

Because scouring of polychaete habitat to decrease *C. shasta* spore concentration is a major goal of the Proposed Action, we modeled the hypothesized effect of the Proposed Action on *C. shasta* spore concentrations. Based on findings of field monitoring data for polychaetes and *C. shasta* spores, we hypothesized that flushing flows of the magnitude and duration defined in the Proposed Action would both delay the timing of when spore concentration exceeded 0 spores/L and decrease spore concentrations proportionally to the expected reduction in polychaete populations.

First, to model the delay in onset of spore concentrations greater than 0 spores/L, the Bureau of Reclamation (2018) reported that the spore concentrations exceeded 0 spores/L roughly 1 month after flows on the descending limb of a spring hydrograph decreased to less than 6,000 ft^3/s, with the lag time in dryer years shortening to roughly 3 weeks. To model this observed phenomenon for the PA scenario, we set spore concentration to 0 for 25 days following the last day in which Iron Gate discharge exceeded 6,030 ft^3/s on the descending limb of the hydrograph.

We then used polychaete monitoring data to estimate the expected reduction in polychaete populations and spore concentration in response to the Proposed Action. One year (2018) of data was used to infer changes in polychaete density associated with the 3-day event of 6030 ft^3/s targeted by surface flushing flows. In several years, attempts had been made to modify the sampling schedule to more specifically capture the effects of other like-discharge events, but safety issues hampered the ability to effectively collect the required data. Sampling occurred in other years when index polychaete sampling coincided with flows of this targeted magnitude and duration, but in none of the other years did the combination of before-and-after sampling exist to estimate the effect of the flow event on polychaete populations.

Samples were collected from the three uppermost index sites prior to the flushing flow event (March 1), immediately after the flow event (April 15), and 1 month after the flow event (May 15). These index samples are collected on stable boulder substrates. At all three sites, the density of polychaetes decreased substantially and immediately after the flushing flow event, with densities ranging from 6 to 19 percent of their pre-event levels. One month later, the densities had increased to range from 15 to 25 percent of their pre-event densities, which still represent substantial decreases relative to before the flow events.

Using the most conservative value from the polychaete index sampling, we assumed that polychaete populations would decrease to 25 percent of their pre-event levels in response to the three-dimensional flushing flow of greater than or equal to 6,030 ft^3/s incorporated in the PA scenario. We then modified the HI daily spore concentrations by reducing spore concentrations for the post-onset period to 25 percent of pre-event levels under the hypothesis that the reduction

in spore concentration is directly proportional to the reduction in polychaete population. Finally, because the years 2005, 2006, and 2016 had observed springtime flows meeting or exceeding the magnitude and duration of the PA scenario flushing flows (fig. 2), only the delay in the timing of spore concentration exceeding 0 spore/L was applied for the PA scenario, but no reduction in observed concentrations was applied as was done for other years.

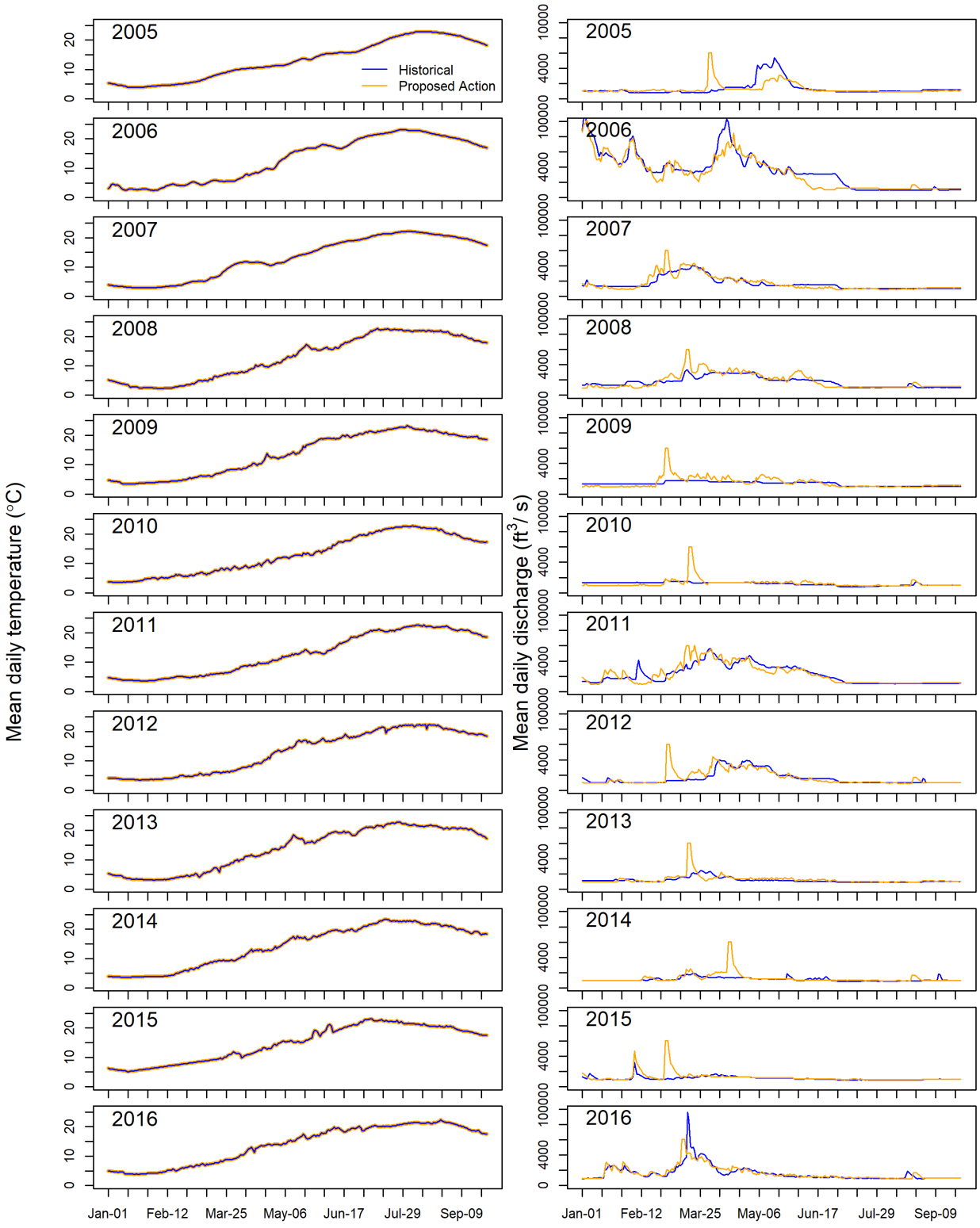

Figure 2. Time series showing mean daily water temperatures (in degrees Celsius [°C]; left graphs) and mean daily river discharge (in cubic feet per second [ft^3/s]; right graphs) by migration year under the Historical and Proposed Action flow management scenarios, at Iron Gate Dam, Klamath River, California, January 1–September 30, 2005–16.

Stream Salmonid Simulator Model Output and Summaries

Although the period of record for the PA scenario was 1981–2016, we could not reconstruct all required model inputs for the period of record. Because regular monitoring of spore concentrations began in 2005, we were able to construct all required model inputs for the HI and PA scenarios for juvenile outmigration years 2005–16 (brood years 2004–14). Therefore, we simulated juvenile Chinook salmon population dynamics between Iron Gate Dam and the ocean for water years 2005–16.

For each year, S3 simulates the daily abundance and mean size of fish in each life stage (fry, parr, and smolt) from each source population in each habitat unit. Because juvenile salmon abundance is tracked both spatially and temporally, the daily abundance of fish passing any given location can be summarized over a day, week, migration season, or year. To show the difference in scenarios, we used two locations in the Klamath River as benchmarks from which to compare the effect of each scenario on juvenile salmon abundance and survival. These locations were (1) the Kinsman Creek trap site (rkm 236.08) and (2) the Pacific Ocean (rkm 0). The Kinsman Creek trap site is situated at the lower end of the infectious disease zone (see fig. 1), and we used this location for summarizing model output because it is a standard monitoring site where juvenile fish abundance and prevalence of infection with *C. shasta* is routinely monitored each year. However, although the prevalence of infection may be expected to be relatively high in some years, mortality owing to disease may be relatively low because infected fish will have yet to succumb to the disease. In contrast, quantifying juvenile salmon abundance at the Pacific Ocean indicates the outcome of in-river mortality processes affected by project operations and disease processes, although infected fish that arrive at the ocean alive are presumed to eventually die from *C. shasta*.

Quantifying Juvenile Salmon Abundance and Survival

To compare S3 model output between the HI and PA scenarios, we calculated the annual survival of juvenile salmon using the simulated abundances of fish from each tributary source passing the two benchmark locations. Survival was calculated as the simulated annual fish abundance (N) in year y from tributary source k passing location l under scenario f, divided by the initial annual abundance of fish that emerged as fry within the Klamath River or that entered the Klamath River from tributaries (N_T):

$$S_{yklf} = \frac{N_{yklf}}{N_{T\,yklf}} . \tag{2}$$

This calculation allows for the comparison of annual survival for fish originating from different tributary and hatchery sources that passed the benchmark locations under either the HI or PA scenario.

Interpreting In-River Mortality and Disease Prevalence

To quantify the prevalence of infection (*POI*) from S3 model output, we divided the simulated annual abundance of infected fish (*I*) in year *y* that originated from tributary source *k* and passed location *l* under scenario *f* by the total annual abundance (*N*):

$$POI_{yklf} = \frac{I_{yklf}}{N_{yklf}} . \quad (3)$$

This calculation allows for the comparison of the fraction of infected fish that originated from different tributary and hatchery sources at a specific location of the Klamath River under either the HI and PA scenarios. To provide a relative estimate of the difference in survival and infected fish at the ocean, we calculated the percent change in the PA scenario relative to the HI scenario, by taking the difference (in either *POI* or *S*) between the PA and HI scenarios (PA-HI) and dividing by the corresponding value (*POI* or *S*) under the HI scenario.

Understanding how the S3 disease model works is important for interpreting in-river mortality, the prevalence of infection at ocean entry, and the differences among the scenarios. The disease model that has been incorporated in the S3 model is based on analysis of extended sentinel trials where exposure times of juvenile salmon to *C. shasta* were varied from 1 to 7 days. The S3 disease model (estimated from the extended sentinel data) comprises two parts: (1) The probability of becoming infected and dying owing to *C. shasta*, and (2) the time from initial exposure to death. The first part of the model predicts the proportion of fish that will eventually die from *C. shasta*, which is estimated from the total mortality observed in each sentinel trial. In S3, the first part of the model transitions fish from non-infected to infected fish that will eventually die but are not yet dead. In the second part, infected fish die based on the time lag between initial exposure and eventual death (Perry and others, 2019).

When evaluating scenarios, both the difference in survival and prevalence of infection should be taken into account because infected fish are those that would be expected to eventually die based on our modeling of the extended sentinel experiments. For example, the prevalence of infection at ocean entry indicates fish that would be expected to eventually die, but their time to death was such that they arrived at the ocean before death occurred. Migration rates in S3 are driven, in turn, by (1) fish size (which, in turn, is affected by water temperature and fish growth rates), and (2) habitat availability and fish density. Therefore, whether infected fish die in-river because of disease depends on the interplay between their predicted time-to-death and population-specific migration rates.

Estimation of Adult Equivalents

We convert juveniles at ocean entry to the number of adult equivalents using estimates of age-specific ocean survival rates from Hankin and Logan (2010). This information may be useful to resource managers concerned with the contribution of Klamath River salmon to marine mammals such as killer whales. First, we obtained an estimate of mean survival from release (R) at Iron Gate Hatchery to age 2 in the Pacific Ocean ($S_{R\text{-}2} = 0.01043$; Hankin and Logan, 2010).

Using the median survival of Iron Gate Hatchery fish from release to the ocean simulated by S3 ($S_{R\text{-}O} = 0.31$), we then back-calculated the expected survival from ocean entry to age 2 in the ocean:

$$S_{\text{O-2}} = \frac{S_{\text{R-2}}}{S_{\text{R-O}}}, \tag{4}$$

which yielded an estimate of $S_{\text{O-2}} = 0.03325$. Next, we used the estimates of ocean survival from ages 2 to 3 ($S_{2\text{-}3} = 0.5$) and ages 3 to 4 ($S_{3\text{-}4} = 0.8$) from Hankin and Logan (2010) to calculate age-4 adult equivalents from juvenile abundance at ocean entry:

$$A_{yklf} = N_{yklf} \cdot S_{O-2} \cdot S_{2-3} \cdot S_{3-4}. \tag{5}$$

Results

Stream Salmonid Simulator Inputs

River Flows, Water Temperatures, and *Ceratonova shasta* Spore Concentrations

Mean daily water temperatures increased with the progression of summer regardless of the scenario; water temperatures at Iron Gate Dam for both management scenarios were virtually identical across the years (fig. 2). From January 1 to September 30, daily Klamath River temperatures at Iron Gate Dam varied from a low of 2.3° C to a high of 23.4 °C across the years and scenarios. The median of daily river temperatures was highest in migration year 2014 at 16.8° C.

Mean daily river discharge was much more variable between the years and management scenarios than water temperature (fig. 2). The lowest median river flows were measured during the 2015 migration year under the HI scenario (median flow at Iron Gate Dam = 991 ft^3/s), yet the highest river flows for the longest duration were measured in the 2006 migration year (peak flow at Iron Gate Dam = 11,100 ft^3/s). Median river discharge was, on average, higher under the HI scenario (mean difference = -101 ft^3/s), whereas peak river flows were, on average, higher under the PA scenario (mean difference = 1,874 ft^3/s). This was especially apparent during low-flow years, where maximum flow peaks (6,030 ft^3/s) prescribed under the PA scenario were the maximum annual flow at the dam.

From January 1 to September 30, concentrations of *C. shasta* spores varied by migration year, but in all years both median and maximum spore concentrations were lower during the PA scenario compared to the HI scenario (fig. 3). Six years had high spore concentrations (>10 spores/L) that likely caused measurable disease effects: 2007, 2008, 2009, 2014, 2015, and 2016. The 2015 migration year had the highest spore concentrations over the period of record regardless of the management scenario. Simulated spore concentrations typically were lower over the entire migration season for juvenile salmon under the PA scenario owing to the hypothesized effect of flushing flows on *C. shasta* spore concentrations. The annual medians of daily spore concentrations were only slightly higher under the HI scenario (mean difference = -3.6 spores/L), but maximum spore concentrations were much higher under the HI scenario (mean difference = -101.9 spores/L).

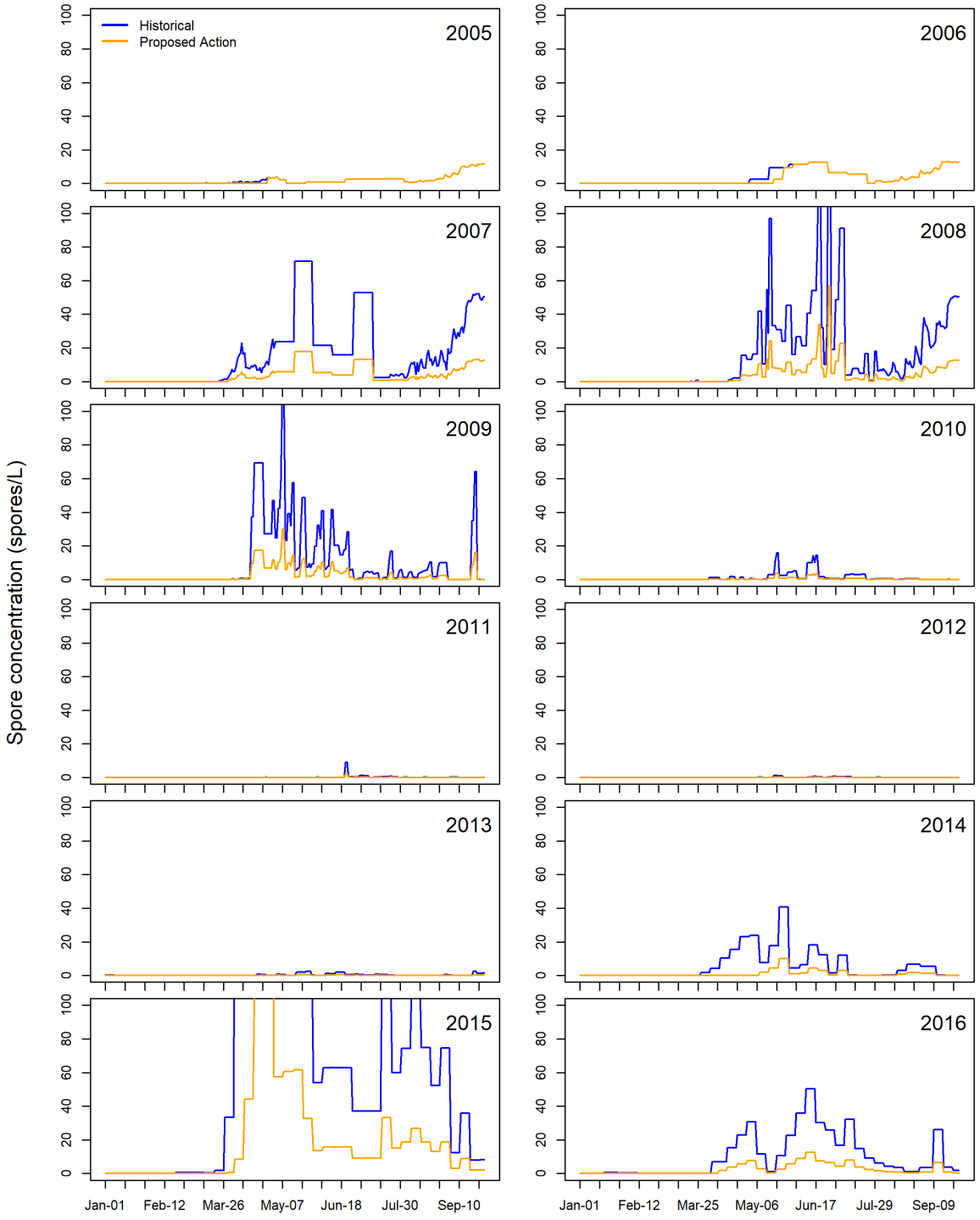

Figure 3. Time series showing mean daily spore concentrations for a given migration year and management scenario in the disease zone of the Klamath River, California, January 1–September 30, 2005–16. Concentrations are given in spores per liter (spores/L) and the y-axis is truncated at 100 spores/L.

Klamath River Spawners and Juveniles Entering from Tributaries

The number of female spawners in the main-stem Klamath River downstream of Iron Gate Dam varied widely among brood years (table 1). In 2010, there were 1,947 spawning females, but in 2012, there were 10,624 spawning females. The spatial distribution of spawners was very consistent from year to year, with most redds located in areas of the Klamath River just downstream from Iron Gate Dam (Gough and others, 2015). The within-year temporal distribution of spawning also was consistent across the years, with 20th- and 80th-percentile spawning dates falling within about 2-weeks from each other (table 1). For example, the 20th percentile spawning dates ranged from October 7 to 25, the 50th percentiles ranged from October 18 to November 5, and the 80th percentiles ranged from October 23 to November 4.

Table 1. Annual female Chinook salmon spawner abundance and spawn timing based on Historical annual abundance estimates, Klamath River downstream of Iron Gate Dam, California, 2004–15.

[Number and timing of spawning fish used as Stream Salmonid Simulator model inputs were identical among scenarios]

Brood year	Percentile spawning dates			Female spawners
	20 percent	50 percent	80 percent	
2004	October 15	October 21	October 29	2,866
2005	October 11	October 18	October 23	2,245
2006	October 7	October 14	October 23	2,018
2007	October 25	November 5	November 14	4,499
2008	October 19	October 25	November 1	3,163
2009	October 16	October 25	November 2	3,980
2010	October 18	October 28	November 5	1,947
2011	October 18	October 28	November 4	2,174
2012	October 14	October 21	October 27	10,624
2013	October 17	October 24	October 31	7,021
2014	October 19	October 25	November 3	10,279
2015	October 13	October 21	October 30	4,028

The total abundance of juvenile salmon entering the Klamath River from tributaries varied widely across source populations and years (table 2). For example, in 2012, 160,530 juvenile Chinook salmon entered the Klamath River from the Shasta River, but in 2012, 6,496,586 fish entered the Klamath River from Bogus Creek located adjacent to the Iron Gate Hatchery. On average across all years, the fraction of juvenile Chinook salmon entering the Klamath River from each source tributary was 43 percent from the Klamath River, 20 percent from Iron Gate Hatchery, 13 percent from Bogus Creek, 1 percent from the Salmon River, 2 percent from the Scott River, 8 percent from the Shasta River, 3 percent from the Trinity River Hatchery, and 11 percent from the Trinity River. Because of the high number of returning spawning females to the Klamath River during 2012–14, there was large production of juvenile salmon from the main-stem Klamath River in migration years 2013–15. Therefore, our modeling includes a wide range of variation in the number spawning females and tributary juveniles from which to simulate and assess the PA and HI scenarios.

Table 2. Annual simulated abundance of emerging fry in Klamath River, and number of juvenile Chinook Salmon entering the Klamath River from tributary and hatchery sources (in millions), California, 2005–16.

[Emerging fry were simulated from the abundance of spawners by S3, whereas juveniles entering from tributaries were included as model inputs. Because of high flows, estimates of Trinity River fish entering the Klamath River were not available during 2006 (as indicated by symbol –)]

Migration year	Klamath River	Klamath hatchery	Bogus Creek	Salmon River	Scott River	Shasta River	Trinity hatchery	Trinity River
2005	6.113	5.370	1.250	0.032	0.179	0.296	0.669	2.399
2006	4.650	6.172	0.189	0.080	0.011	0.083	–	–
2007	4.275	5.364	1.895	0.098	0.435	0.580	0.479	1.869
2008	9.080	5.313	3.039	0.116	0.552	0.989	0.362	2.623
2009	6.770	0.993	1.757	0.140	0.930	0.724	0.775	2.965
2010	8.555	4.528	5.450	0.157	0.640	2.348	1.223	3.539
2011	4.154	3.938	1.197	0.204	0.119	0.655	0.874	2.824
2012	4.597	5.032	6.497	0.211	0.170	0.161	0.425	5.322
2013	20.770	4.223	5.398	0.158	0.655	5.218	0.368	4.763
2014	14.477	4.427	2.500	0.167	0.423	4.734	0.334	2.477
2015	22.583	3.827	5.795	0.140	0.243	2.902	0.634	0.882
2016	9.015	3.647	0.832	0.086	0.059	2.758	0.737	0.789

Stream Salmonid Simulator Output

Ceratonova shasta Infection and Mortality

The timing of migration influenced exposure to *C. shasta* and subsequent infection rates of fish from different tributary sources under each scenario. Among tributaries, fish from the Shasta River tended to have peak migration dates earlier than other populations, which often coincided with lower spore concentrations (figs. 4 and 5). Releases of hatchery fish often occurred much later than migration of natural populations, which sometimes exposed hatchery fish to higher spore concentrations than natural populations (for example, in 2008) and sometimes exposed them to lower spore concentrations (for example., in 2009; figs. 4 and 5).

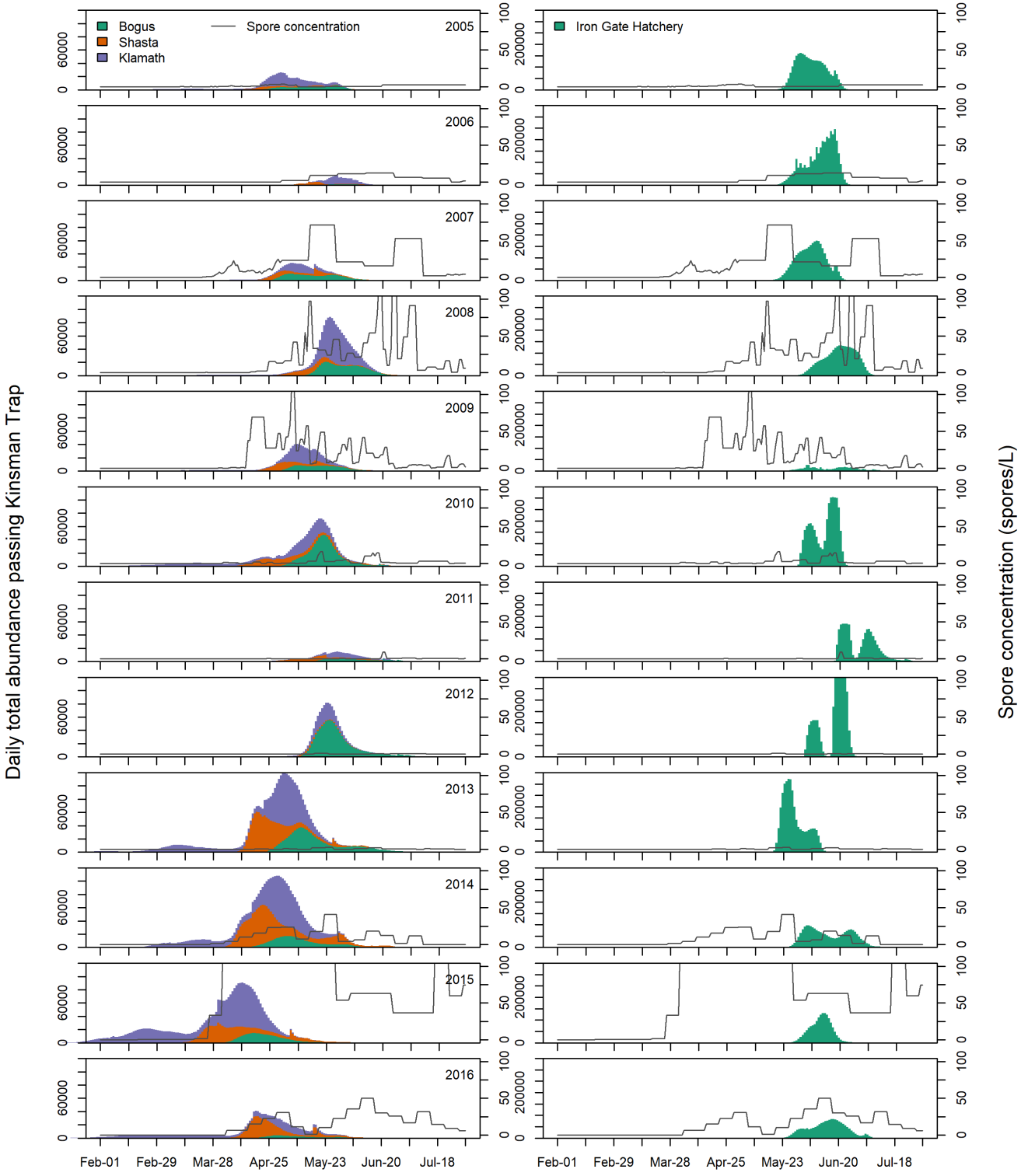

Figure 4. Stacked bar charts showing daily abundance of juvenile Chinook salmon, under Historical scenario, migrating past the Kinsman Creek trap site, Klamath River Basin, California, 2005–16. Solid line shows spore concentration (in spores per liter [spores/L]; second y-axis). Left column shows naturally produced juveniles and right column shows hatchery-origin juveniles. Bogus, Bogus Creek; Shasta, Shasta River; Klamath, Klamath River.

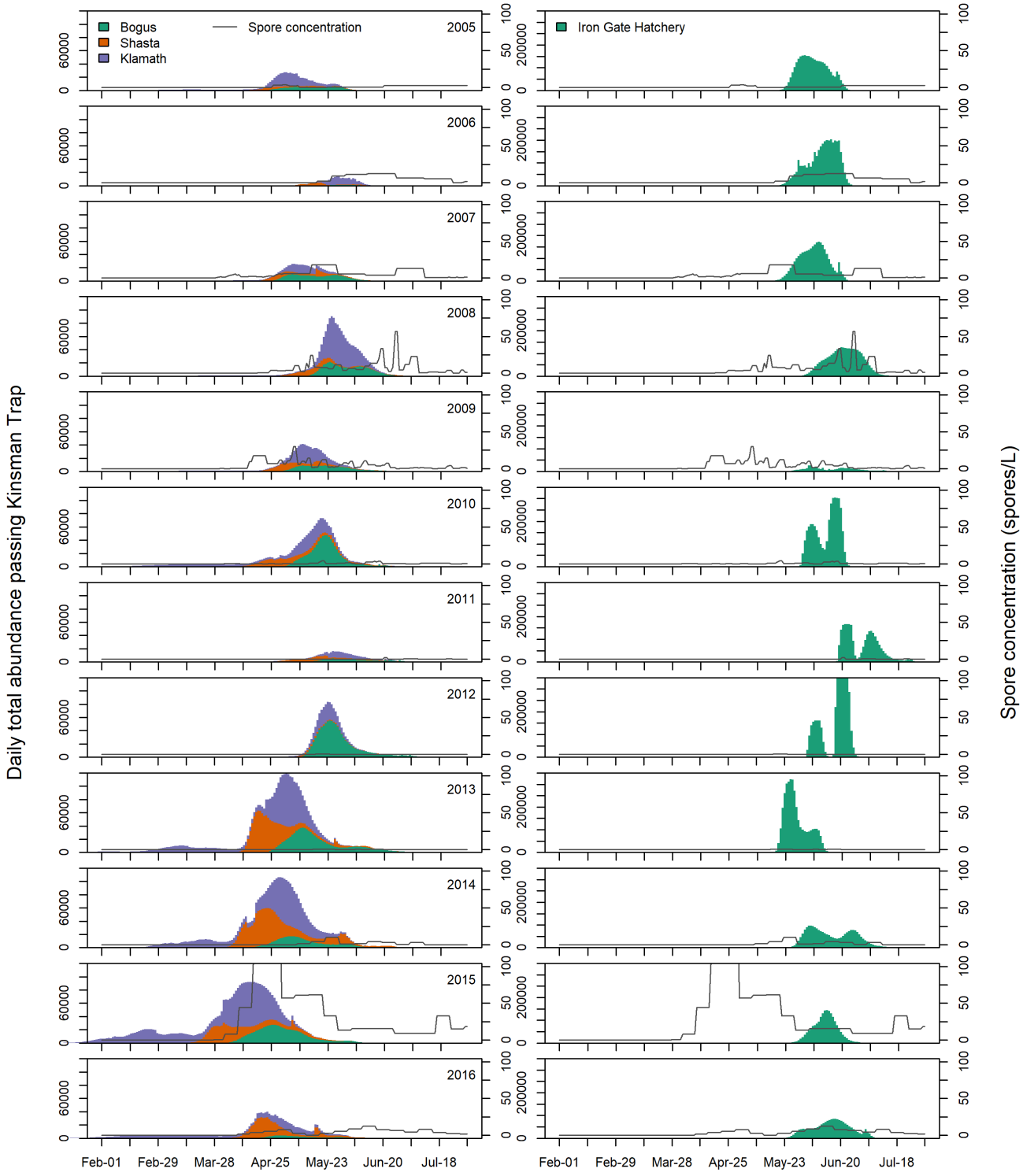

Figure 5. Stacked bar charts showing daily abundance of juvenile Chinook salmon, under Proposed Action scenario, migrating past the Kinsman Creek trap site, Klamath River Basin, California, 2005–16. Solid line shows spore concentration (in spores per liter [spores/L]; second y-axis). Left column shows naturally produced juveniles and right column shows hatchery-origin juveniles. Bogus, Bogus Creek; Shasta, Shasta River; Klamath, Klamath River.

Migration timing combined with simulated management actions directly influenced infection prevalence. For example, simulated infection prevalence under the HI scenario was high during the 6 years with high spore concentrations (2006–09 and 2014–16; fig. 4). Although spore concentrations were hypothesized to be lower under the PA for all years, the timing of flushing flows influenced when spore concentrations exceeded 0 spores/L, which in turn influenced the magnitude of infection prevalence in some years more than others. For example, the mid-April timing of a surface flushing-flow event in 2014 (fig. 2) is assumed to have resulted in spore concentrations to remain undetectable for 25 days until early May (fig. 3). Because the timing of the flushing flow in 2014 occurred just a few weeks prior to the outmigration of juvenile salmon through the infectious zone, infection prevalence during April under the PA scenario was considerably lower than under the HI scenario (figs. 6 and 7). In contrast, flushing flows in 2015 occurred in late February (fig. 2), which had little effect on the timing and increase in spore concentrations (fig. 3). Although spore concentrations in 2015 decreased under the PA scenario (fig. 5), they remained well above the 10-spores/L threshold known to increase infection rates. Thus, both the timing of flushing flows and magnitude of spore concentrations in 2015 led to relatively little difference in infection prevalence between scenarios (figs. 6 and 7) relative to the difference observed in 2014.

Similar to prevalence of infection, the spatial distribution and magnitude of mortality caused by *C. shasta* also varied among years and scenarios. We noted that mortality owing to *C. shasta* was distributed far downstream of the infectious zone owing to the lag time between *C. shasta* exposure and death (figs. 8 and 9). However, in some years (for example, 2015), higher mortality occurred in the infectious zone because the time to death of infected fish is affected by water temperature, spore concentration, and exposure duration. Among scenarios, mortality under the PA scenario was less than under the HI scenario, particularly in 2014 (figs. 8 and 9).

Annual prevalence of infection (*POI*) at the Kinsman Creek trap varied among populations passing the trap and between scenarios (figs. 10 and 11). Among populations, maximum *POI* ranged from about 0.45 for the Shasta River to 0.6 for offspring of the Klamath River main-stem spawners (fig. 10). Although *POI* was always high in years when spore concentrations were high, *POI* was consistently lower under the PA scenario (fig. 10). Aggregated across naturally produced populations, the highest annual *POI* occurred in 2008 under the HI scenario (about 0.65 *POI*), and the largest difference in *POI* between scenarios occurred in 2014 (about 0.1 for PA compared to 0.4 for HI; fig. 11).

Estimates of *POI* for simulated juvenile salmon that arrived at the ocean had a pattern that differed from that at the Kinsman Creek trap site owing to in-river mortality of infected fish (figs. 10 and 12). *POI* for fish arriving at the ocean often was higher under the PA scenario compared to the HI scenario (fig. 12). This result largely was due to the amount of in-river mortality expressed under each of the scenarios. Under the HI scenario, fish were exposed to much higher spore concentration, which greatly increased infection rates, shortened their time to death, and increased the amount of in-river mortality for fish exposed to the infectious disease zone (table 3 and fig. 12) as compared to the PA scenario. Thus, under the HI scenario, fish suffered greater mortality before arriving at the Pacific Ocean. Therefore, *POI* values were higher for juvenile salmon at the Pacific Ocean under the PA scenario than the HI scenario because a larger fraction of infected fish survived to ocean entry (fig. 13).

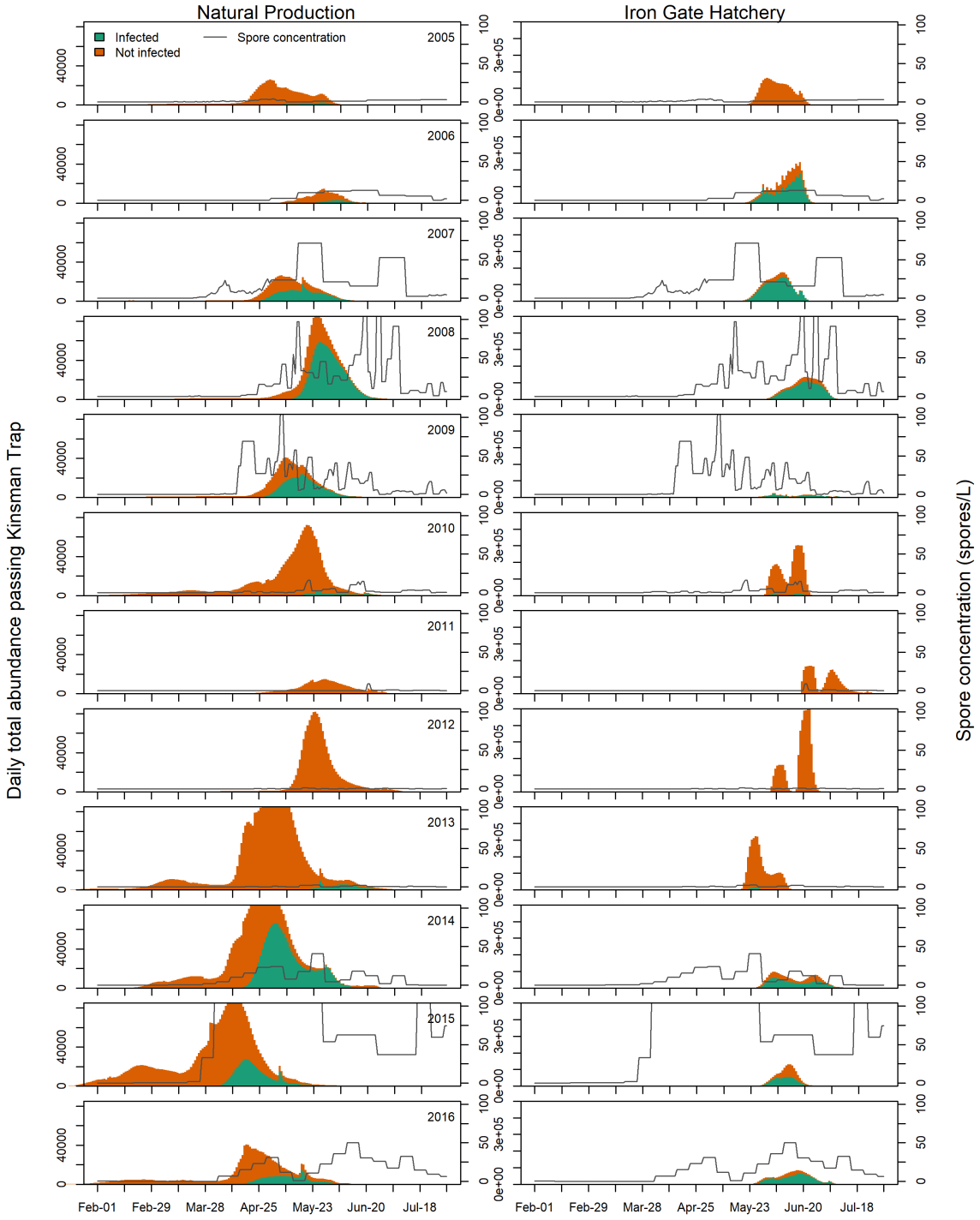

Figure 6. Stacked bar charts showing daily abundance of uninfected and *Ceratonova shasta*-infected juvenile Chinook salmon, under Historical scenario, migrating past the Kinsman Creek trap site, Klamath River Basin, California, 2005–16. Solid line shows spore concentration (in spores per liter [spores/L]; second y-axis). Left column shows naturally produced juveniles and right column shows hatchery-origin juveniles.

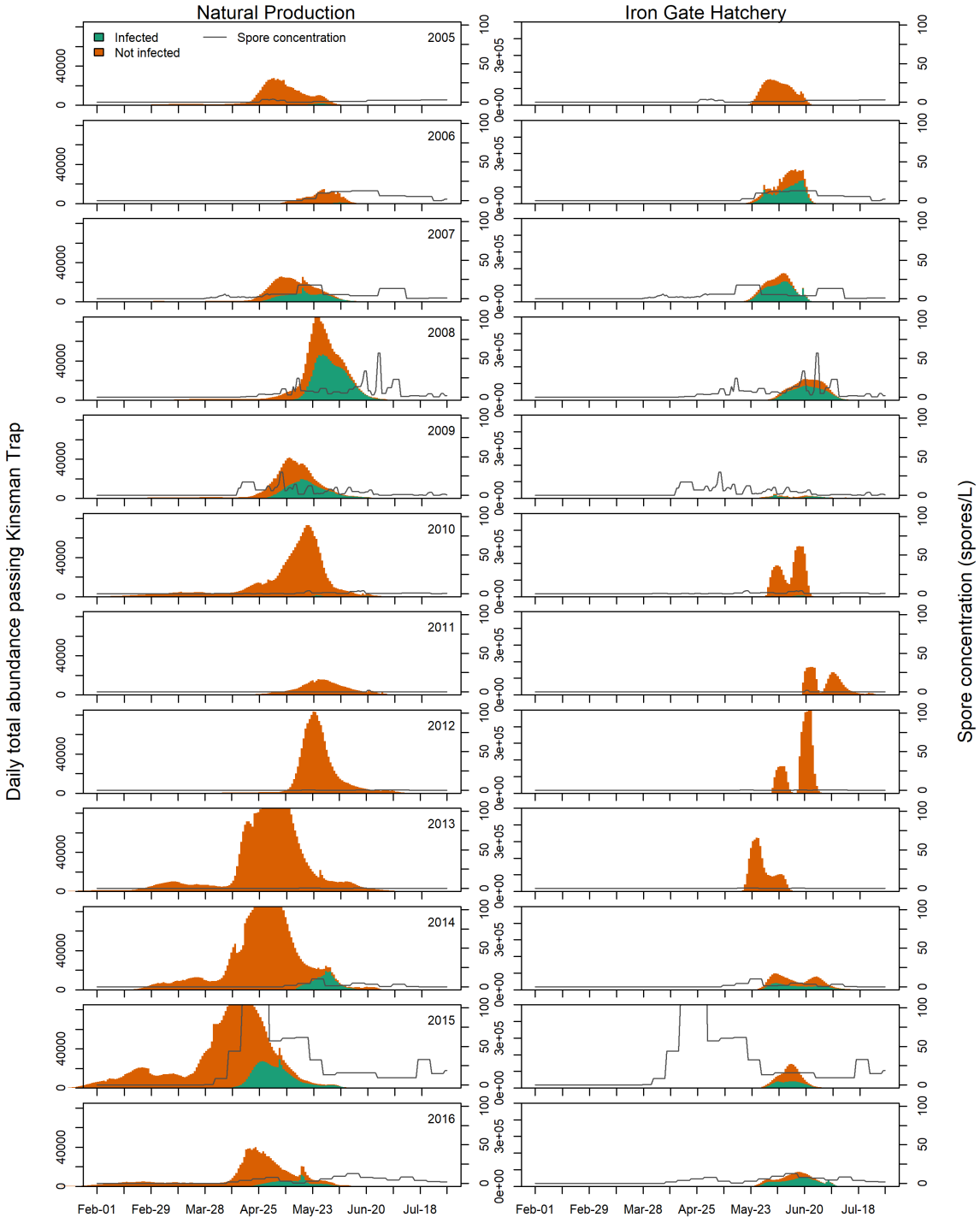

Figure 7. Stacked bar charts showing daily abundance of uninfected and *Ceratonova shasta*-infected juvenile Chinook salmon, under Proposed Action scenario, migrating past the Kinsman Creek trap site, Klamath River Basin, California, 2005–16. Solid line shows spore concentration (in spores per liter [spores/L]; second y-axis). Left column shows naturally produced juveniles and right column shows hatchery-origin juveniles.

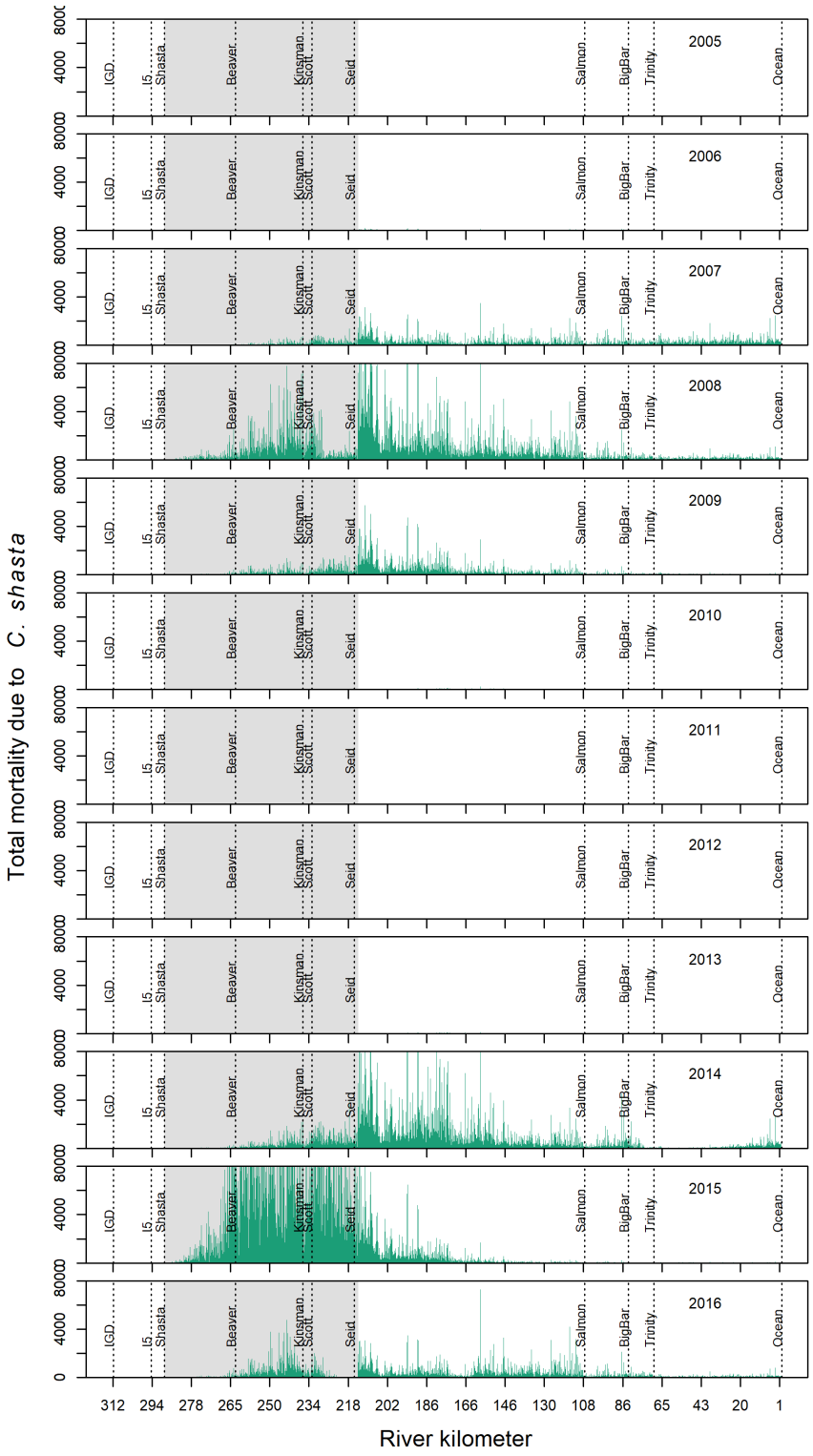

Figure 8. Graphs showing spatial distribution of mortality caused by *Ceratonova shasta* (*C. shasta*) for naturally produced juvenile Chinook salmon, under Historical scenario, migrating past the Kinsman Creek trap site, Klamath River Basin, California, 2005–16. Gray shaded region shows location of the *C. shasta* infectious zone and vertical dashed lines show locations of major tributaries and other landmarks.

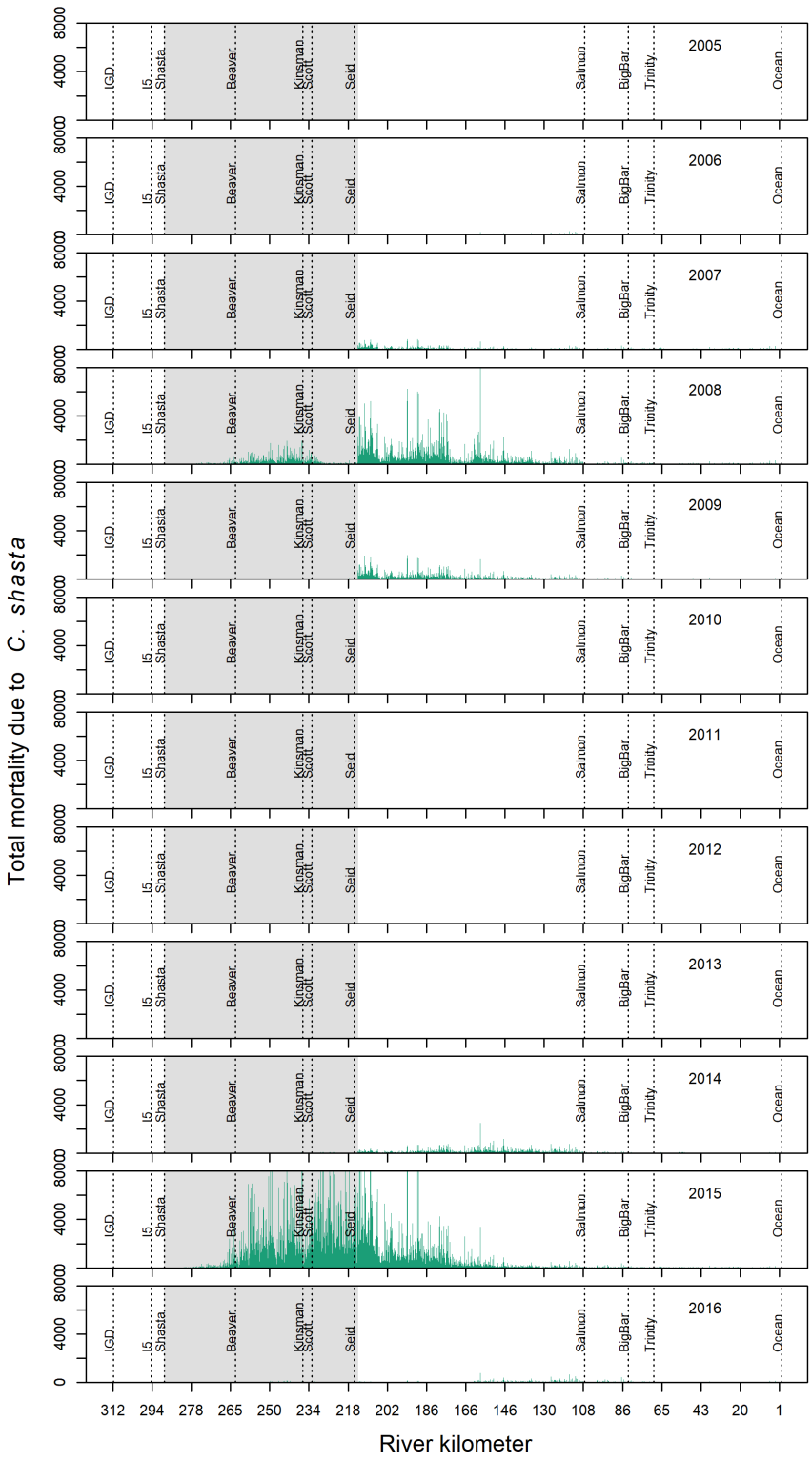

Figure 9. Graphs showing spatial distribution of mortality cause by *Ceratonova shasta* (*C. shasta*) for naturally produced juvenile Chinook salmon, under Proposed Action scenario, migrating past the Kinsman Creek trap site, Klamath River Basin, California, 2005–16. Gray shaded region shows location of the *C. shasta* infectious zone and vertical dashed lines show locations of major tributaries and other landmarks.

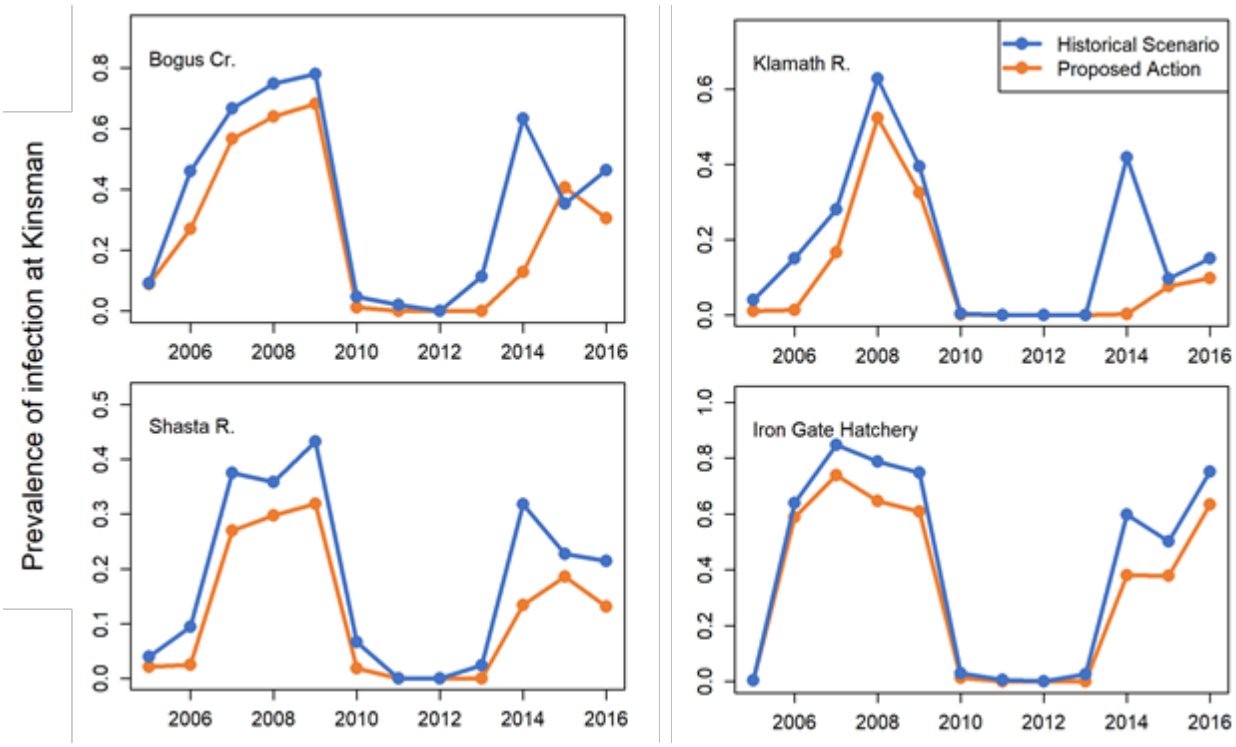

Figure 10. Graphs showing annual prevalence of *Ceratonova shasta* infection simulated by the Stream Salmonid Simulator model for juvenile fall Chinook salmon by tributary and hatchery sources, migration year, and scenario, at the Kinsman fish trap, Klamath River Basin, California, 2005–16. Cr., Creek; R., River.

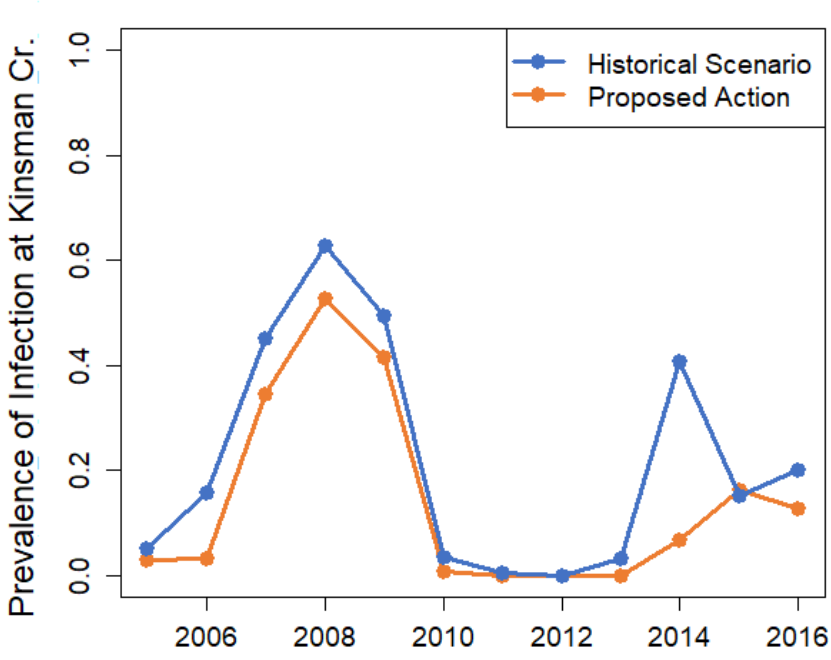

Figure 11. Graph showing annual prevalence of *Ceratonova shasta* infection simulated by the Stream Salmonid Simulator model for all naturally produced populations of juvenile fall Chinook salmon, by migration year and scenario, passing the Kinsman fish trap, Klamath River Basin, California, 2005–16. Cr., Creek.

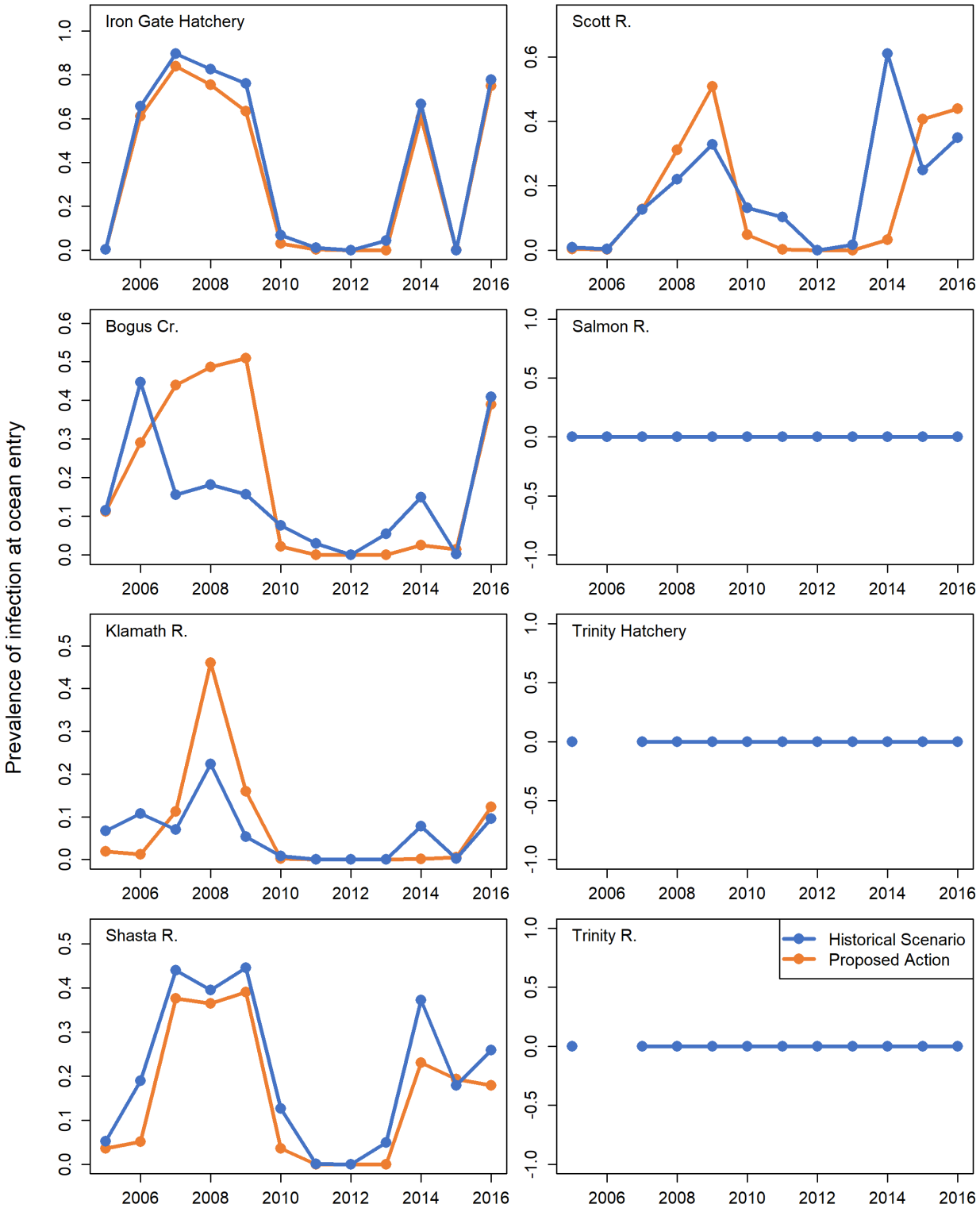

Figure 12. Graphs showing prevalence of *Ceratonova shasta* infection simulated by the Stream Salmonid Simulator model for juvenile fall Chinook salmon by tributary and hatchery sources, migration year, and scenario, at the Pacific Ocean, California, 2005–16. Cr., Creek; R., River.

Table 3. Abundance of juvenile fall Chinook salmon infected by *Ceratonova shasta* as simulated by the Stream Salmonid Simulator model under the Historical and Proposed Action scenarios, at entry to the Pacific Ocean, California, 2005–16.

[Because of high flows, estimates of Trinity River fish entering the Klamath River were not available during 2006 (as indicated by symbol –)]

Migration year	Klamath River	Klamath hatchery	Bogus Creek	Salmon River	Scott River	Shasta River	Trinity hatchery	Trinity River	Annual total
Historical									
2005	7,675	6,438	6,842	0	531	2,357	0	0	23,843
2006	7,519	1,513,501	3,123	0	24	7,587	–	–	1,531,754
2007	5,602	1,403,358	5,584	0	13,151	34,660	0	0	1,462,356
2008	35,857	821,456	7,530	0	4,790	33,690	0	0	903,322
2009	6,175	148,445	2,965	0	9,289	39,005	0	0	205,879
2010	1,524	178,038	17,268	0	4,227	15,268	0	0	216,324
2011	0	18,186	1,541	0	1,101	66	0	0	20,894
2012	0	0	29	0	0	8	0	0	37
2013	3	101,940	11,008	0	1,812	16,250	0	0	131,012
2014	29,417	243,458	7,188	0	14,909	158,819	0	0	453,791
2015	908	0	147	0	2,979	30,464	0	0	34,497
2016	16,786	521,586	11,344	0	694	58,614	0	0	609,023
Proposed Action									
2005	2,266	6,398	6,908	0	255	1,668	0	0	17,494
2006	866	1,390,891	2,239	0	17	2,047	–	–	1,396,059
2007	10,792	1,449,378	31,824	0	12,062	32,864	0	0	1,536,920
2008	136,694	737,494	44,512	0	9,536	33,442	0	0	961,678
2009	23,693	108,712	26,988	0	28,335	39,651	0	0	227,378
2010	332	80,012	4,907	0	1,536	4,309	0	0	91,096
2011	0	3,900	0	0	17	5	0	0	3,923
2012	0	0	0	0	0	0	0	0	0
2013	0	0	0	0	0	0	0	0	0
2014	754	350,137	2,470	0	1,205	108,557	0	0	463,123
2015	2,742	0	1,790	0	9,549	38,532	0	0	52,614
2016	23,895	764,311	13,994	0	1,329	41,589	0	0	845,118

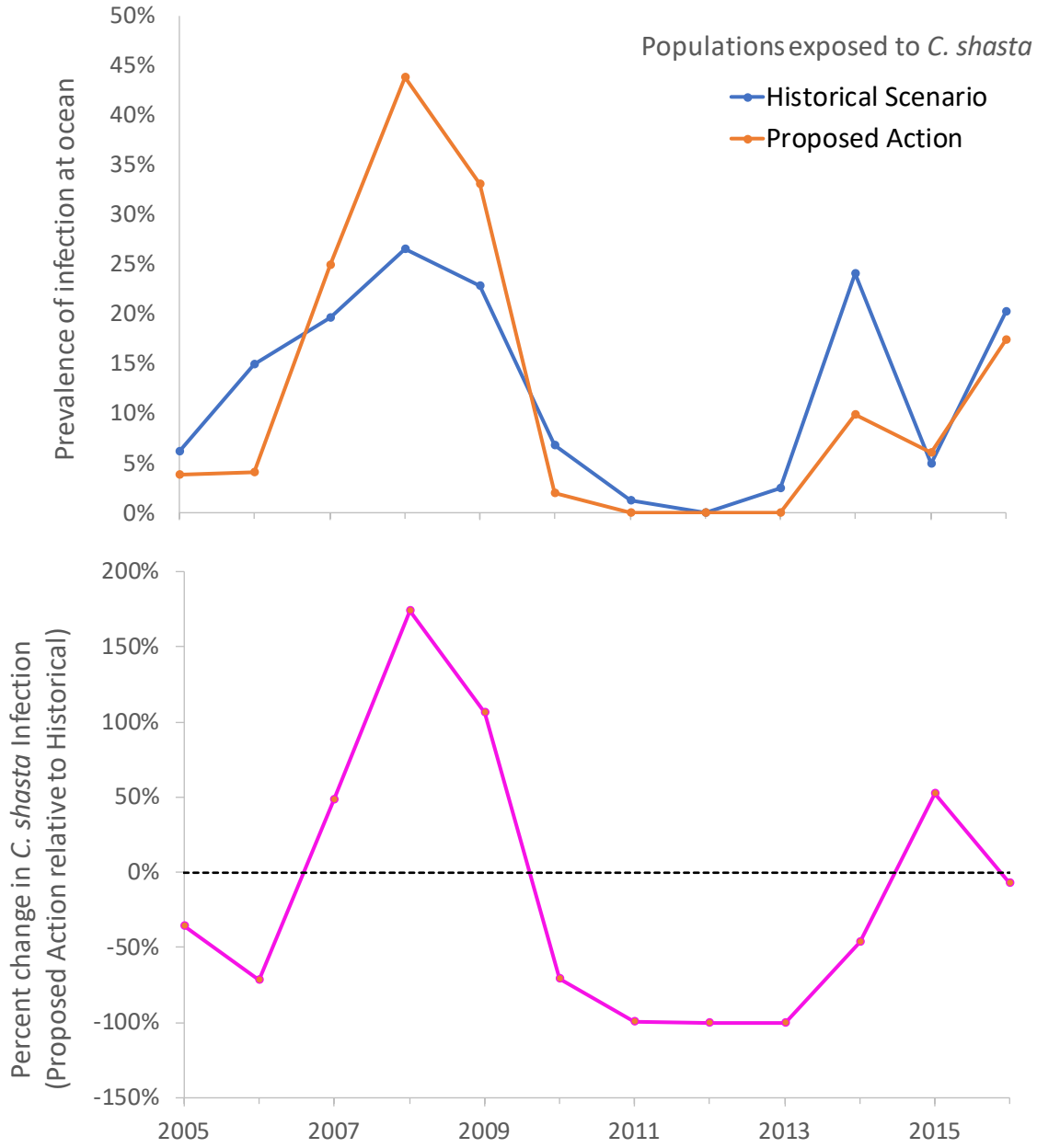

Figure 13. Graphs showing prevalence of *Ceratonova shasta* (*C. shasta*) infection simulated by the Stream Salmonid Simulator model for juvenile fall Chinook salmon at the Pacific Ocean (top graph) and the percent (%) change in prevalence of infection (bottom graph), California, 2005–16. Estimates are combined for the tributary source populations that were exposed to the disease zone: Klamath River, Bogus Creek, Scott River, and Shasta River.

Juvenile Salmon Survival

Survival of juvenile salmon to the Kinsman Creek trap site was similar between the HI and PA scenarios (table 4). Across all years and scenarios, annual survival of simulated fish to the Kinsman Creek trap site varied from 0.042 to 0.918. Under the HI scenario, mean survival across all years to Kinsman Creek trap site was about 8 percent for Klamath River fish, about 62 percent for Klamath River Hatchery fish, about 13 percent for Bogus Creek fish, and about 30 percent for Shasta River fish. Similarly, under the PA scenario, mean survival across all years to Kinsman Creek trap site was about 8 percent for Klamath River fish, about 63 percent for Klamath River Hatchery fish, about 14 percent for Bogus Creek fish, and about 30 percent for Shasta River fish.

Table 4. Juvenile fall Chinook salmon survival, simulated by the Stream Salmonid Simulator model under the Historical and Proposed Action scenarios, to the Kinsman Creek trap site, Klamath River, California, 2005–16.

Migration year	Historical				Proposed Action			
	Klamath River	Klamath hatchery	Bogus Creek	Shasta River	Klamath River	Klamath hatchery	Bogus Creek	Shasta River
2005	0.077	0.567	0.131	0.325	0.076	0.568	0.137	0.317
2006	0.042	0.597	0.100	0.748	0.043	0.602	0.101	0.747
2007	0.069	0.572	0.155	0.314	0.069	0.571	0.157	0.312
2008	0.120	0.522	0.155	0.208	0.119	0.545	0.154	0.204
2009	0.080	0.477	0.137	0.311	0.081	0.470	0.150	0.305
2010	0.087	0.867	0.141	0.158	0.085	0.867	0.141	0.153
2011	0.049	0.639	0.102	0.225	0.051	0.638	0.106	0.228
2012	0.083	0.918	0.151	0.312	0.085	0.918	0.153	0.314
2013	0.084	0.855	0.161	0.205	0.084	0.855	0.162	0.206
2014	0.126	0.513	0.177	0.295	0.123	0.525	0.175	0.288
2015	0.098	0.423	0.059	0.255	0.105	0.506	0.131	0.255
2016	0.068	0.501	0.115	0.217	0.068	0.539	0.114	0.212
Mean	0.082	0.621	0.132	0.298	0.082	0.634	0.140	0.295

The cumulative effect of disease on fish survival from the different tributary source populations is indicated by differences in survival to the Pacific Ocean among populations (table 5, fig. 14). Fish not exposed to the disease zone had very similar survival to the Pacific Ocean between the scenarios, but fish populations exposed to the disease zone had higher survival to the Pacific Ocean under the PA scenario. This was particularly evident for fish that originated from Bogus Creek and the Klamath River during years with high spore concentrations (that is, 2007–09 and 2014–16). For example, the relative increase in survival under the PA scenarios was as high as a 181 percent for Bogus Creek (fig 15).

Table 5. Juvenile fall Chinook salmon survival—simulated by the Stream Salmonid Simulator model under the Historical and Proposed Action scenarios—to the Pacific Ocean, California, 2005–16.

[Because of high flows, estimates of Trinity River fish entering the Klamath River were not available during 2006 (as indicated by symbol –)]

Migration year	Klamath River	Klamath hatchery	Bogus Creek	Salmon River	Scott River	Shasta River	Trinity hatchery	Trinity River
				Historical				
2005	0.019	0.335	0.048	0.069	0.341	0.155	0.651	0.411
2006	0.015	0.373	0.037	0.047	0.514	0.482	–	–
2007	0.019	0.292	0.019	0.080	0.240	0.136	0.575	0.494
2008	0.018	0.187	0.014	0.247	0.039	0.086	0.632	0.569
2009	0.017	0.197	0.011	0.045	0.030	0.121	0.534	0.420
2010	0.022	0.579	0.042	0.229	0.050	0.051	0.749	0.640
2011	0.018	0.377	0.044	0.281	0.090	0.115	0.638	0.547
2012	0.029	0.694	0.053	0.236	0.175	0.163	0.590	0.397
2013	0.026	0.543	0.037	0.038	0.160	0.063	0.304	0.451
2014	0.026	0.083	0.019	0.029	0.058	0.090	0.637	0.612
2015	0.020	0.000	0.010	0.019	0.049	0.059	0.482	0.539
2016	0.019	0.184	0.033	0.122	0.034	0.082	0.571	0.652
Mean	0.021	0.320	0.031	0.120	0.148	0.134	0.530	0.478
				Proposed Action				
2005	0.019	0.335	0.050	0.072	0.344	0.156	0.652	0.412
2006	0.016	0.369	0.041	0.048	0.515	0.481	–	–
2007	0.023	0.322	0.038	0.076	0.217	0.151	0.572	0.492
2008	0.033	0.184	0.030	0.253	0.055	0.093	0.633	0.570
2009	0.022	0.173	0.030	0.043	0.060	0.140	0.524	0.412
2010	0.021	0.579	0.042	0.227	0.050	0.051	0.749	0.640
2011	0.019	0.379	0.044	0.280	0.090	0.115	0.637	0.546
2012	0.030	0.694	0.053	0.237	0.168	0.164	0.589	0.398
2013	0.026	0.548	0.041	0.038	0.191	0.063	0.310	0.453
2014	0.036	0.131	0.039	0.032	0.089	0.100	0.642	0.612
2015	0.023	0.000	0.022	0.019	0.097	0.069	0.484	0.539
2016	0.022	0.280	0.043	0.124	0.052	0.084	0.576	0.655
Mean	0.024	0.333	0.039	0.121	0.161	0.139	0.531	0.477

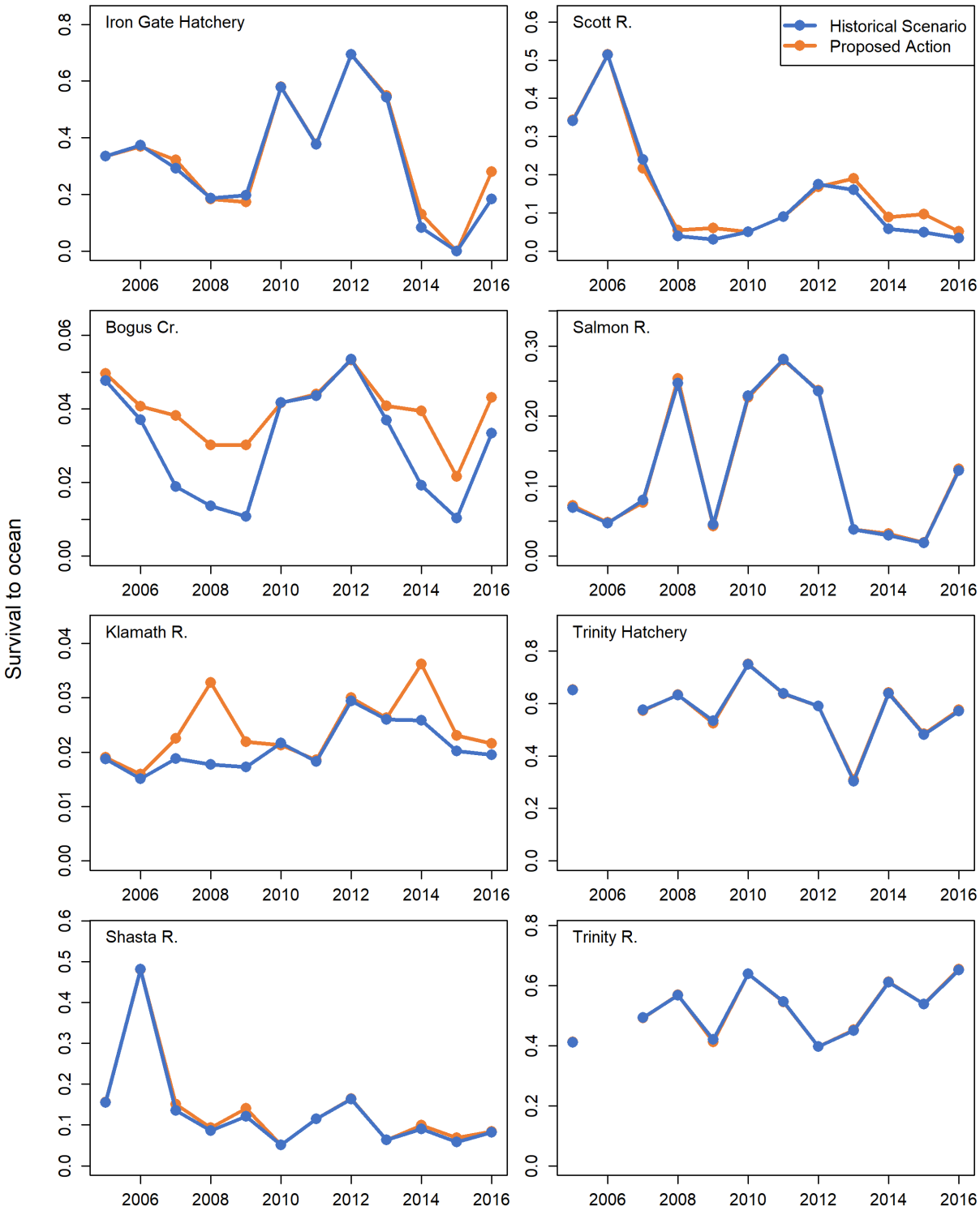

Figure 14. Graphs showing annual juvenile fall Chinook salmon survival (by tributary and hatchery sources, migration year, and scenario) from their entrance (or emergence) into the Klamath River to the Pacific Ocean, California, 2005–16. Cr., Creek; R., River.

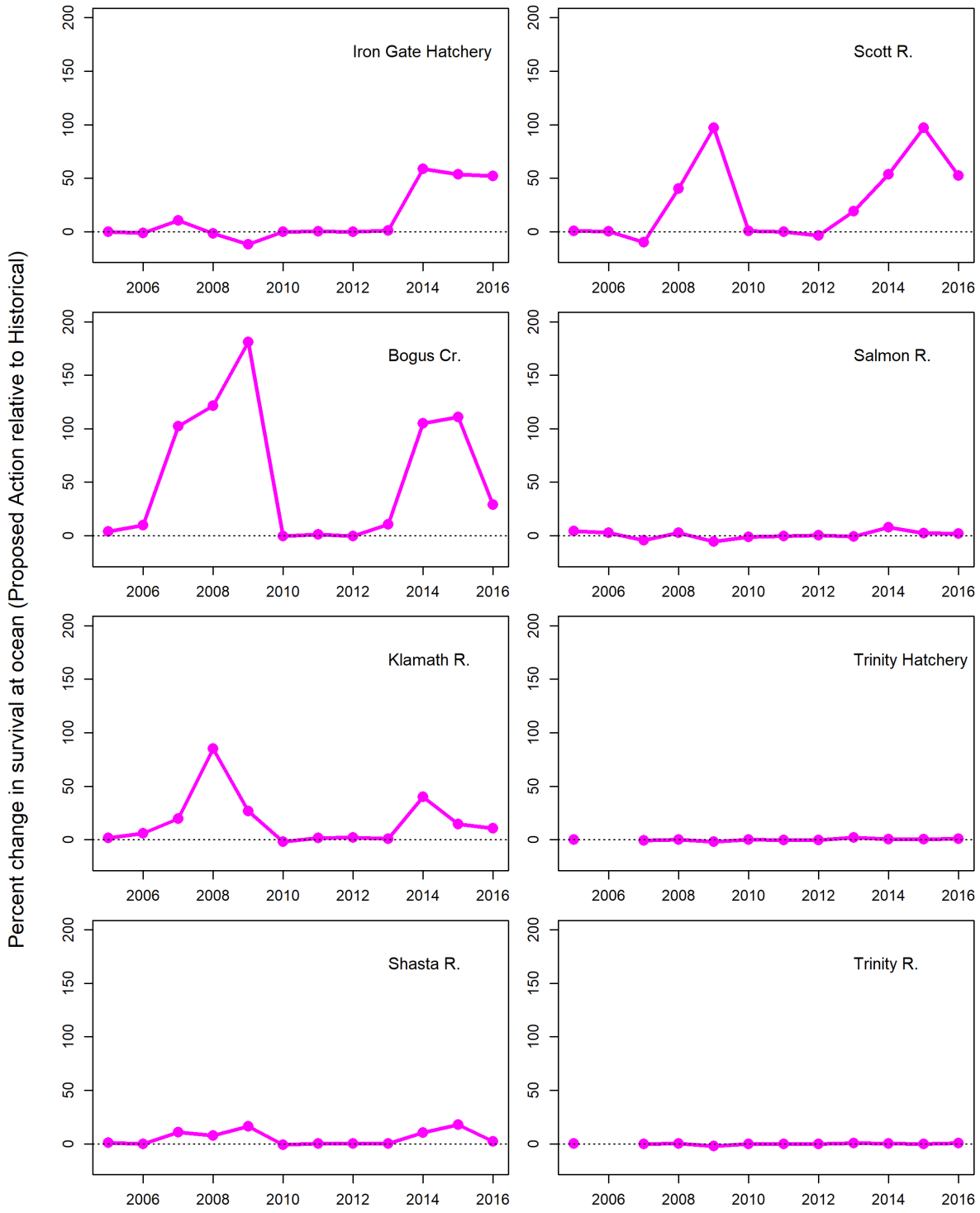

Figure 15. Graphs showing percent change in survival to Pacific Ocean entry for the Proposed Action scenario relative to the Historical scenario for each tributary source population, Klamath River Basin, California, 2005–16. Cr., Creek; R., River.

Juvenile Salmon Abundance

Juvenile salmon abundances at the Kinsman Creek trap site were very similar regardless of the management scenario, but fish abundances for those fish exposed to the disease zone (such as those from Bogus Creek, the Klamath River, and Iron Gate Hatchery) were lower in 2015 compared to other years under the HI scenario (fig. 16). The abundance of juvenile salmon arriving at the Pacific Ocean showed the consequences of having been exposed to the disease zone and subsequent in-river mortality owing to *C. shasta* (table 6, fig. 17). Source populations that migrated through the disease zone showed the largest change in abundance at the ocean. Fish exposed to the disease zone had higher abundance under the PA scenario in years when spore concentrations were high, but in years when spore concentrations were relatively low, similar numbers of fish arrived at the ocean regardless of the scenario. Fish entering the Klamath River from tributaries below the disease zone (Salmon and Trinity Rivers) had similar abundances among the years and scenarios (fig. 17).

Total annual abundance of simulated juvenile salmon at ocean entry ranged from about 0.12 to 1.2 million fish. Under the PA scenario, in high spore concertation years, as much as 259,511 more fish arrived at ocean entry than under the HI scenario (fig. 18), resulting in as much as a 66- percent increase in abundance at the ocean under the PA scenario relative to the HI scenario. Over the time series considered, the scenarios included years with high spore concentrations and relatively low and high juvenile salmon abundances, so the PA scenario appeared to increase juvenile salmon abundances at the ocean in high disease years regardless of juvenile salmon abundance in the river.

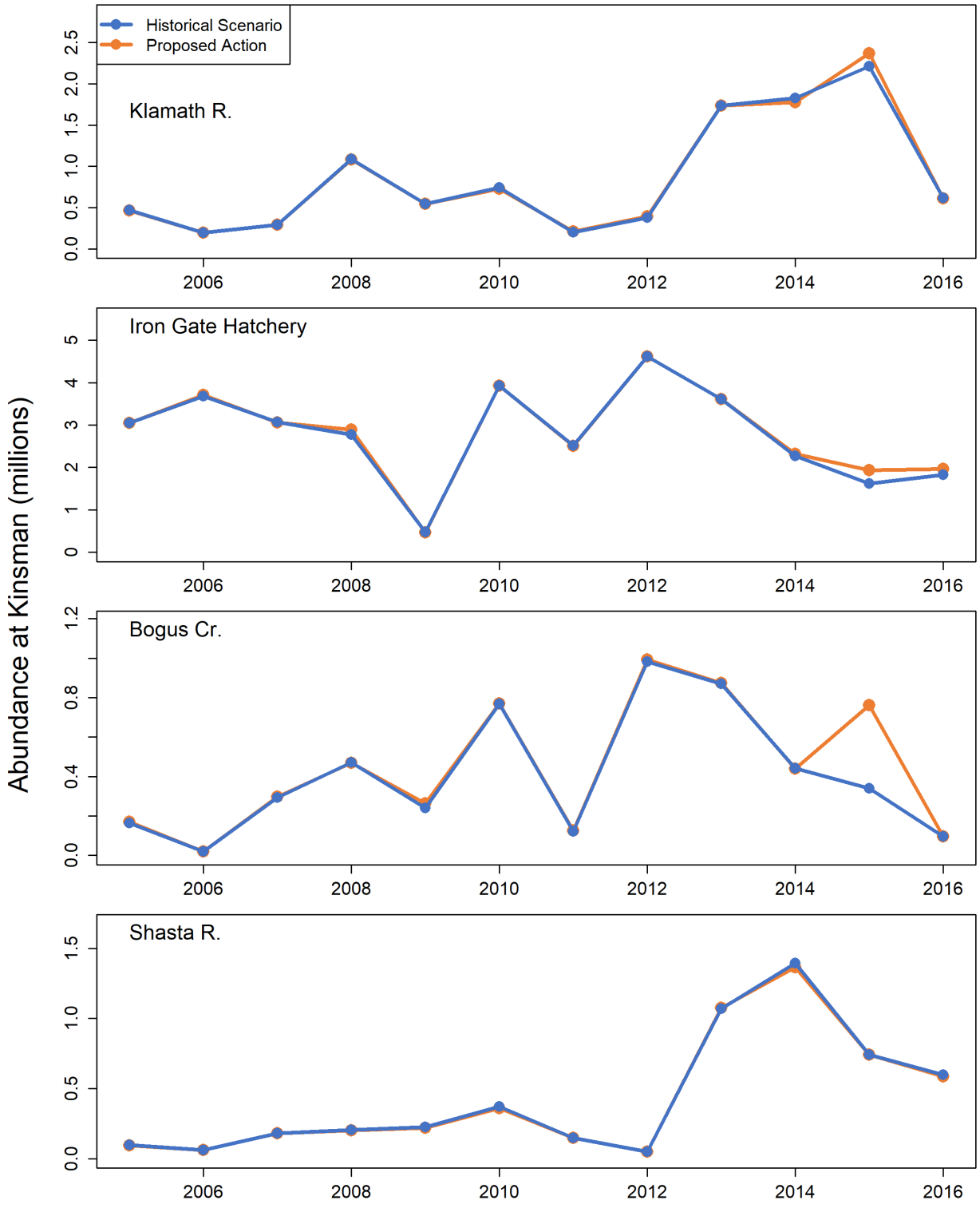

Figure 16. Graphs showing annual juvenile fall Chinook salmon abundances—simulated by the Stream Salmonid Simulator model under the Historical and Proposed Action scenarios—at the Kinsman Creek trap site, Klamath River, California, 2005–16. Cr., Creek; R., River.

Table 6. Annual numbers of juvenile fall Chinook salmon (in millions), as simulated by the Stream Salmonid Simulator model under the Historical and Proposed Action scenarios, arriving at the Pacific Ocean by tributary and hatchery sources to the Klamath River, California, 2005–16.

[Because of high flows, estimates of Trinity River fish entering the Klamath River were not available during 2006 (as indicated by symbol –)]

Migration year	Klamath River	Klamath hatchery	Bogus Creek	Salmon River	Scott River	Shasta River	Trinity hatchery	Trinity River
				Historical				
2005	0.115	1.801	0.060	0.002	0.061	0.046	0.436	0.986
2006	0.070	2.302	0.007	0.004	0.006	0.040	–	–
2007	0.080	1.565	0.036	0.008	0.105	0.079	0.276	0.923
2008	0.160	0.996	0.041	0.029	0.022	0.085	0.229	1.491
2009	0.117	0.195	0.019	0.006	0.028	0.087	0.414	1.246
2010	0.185	2.622	0.227	0.036	0.032	0.121	0.916	2.265
2011	0.076	1.484	0.052	0.057	0.011	0.075	0.558	1.543
2012	0.135	3.493	0.347	0.050	0.030	0.026	0.251	2.115
2013	0.539	2.293	0.199	0.006	0.105	0.330	0.112	2.147
2014	0.376	0.366	0.048	0.005	0.024	0.427	0.213	1.515
2015	0.457	0.000	0.059	0.003	0.012	0.170	0.305	0.475
2016	0.176	0.670	0.028	0.010	0.002	0.227	0.421	0.515
				Proposed Action				
2005	0.117	1.802	0.062	0.002	0.061	0.046	0.436	0.989
2006	0.074	2.277	0.008	0.004	0.006	0.040	–	–
2007	0.096	1.729	0.072	0.007	0.094	0.087	0.274	0.920
2008	0.297	0.978	0.092	0.029	0.031	0.092	0.229	1.494
2009	0.148	0.172	0.053	0.006	0.056	0.102	0.407	1.222
2010	0.182	2.623	0.227	0.036	0.032	0.120	0.916	2.264
2011	0.077	1.492	0.053	0.057	0.011	0.075	0.557	1.541
2012	0.138	3.491	0.346	0.050	0.029	0.026	0.251	2.116
2013	0.545	2.315	0.220	0.006	0.125	0.331	0.114	2.157
2014	0.526	0.580	0.099	0.005	0.038	0.472	0.214	1.517
2015	0.523	0.000	0.125	0.003	0.024	0.200	0.307	0.475
2016	0.194	1.020	0.036	0.011	0.003	0.232	0.424	0.517

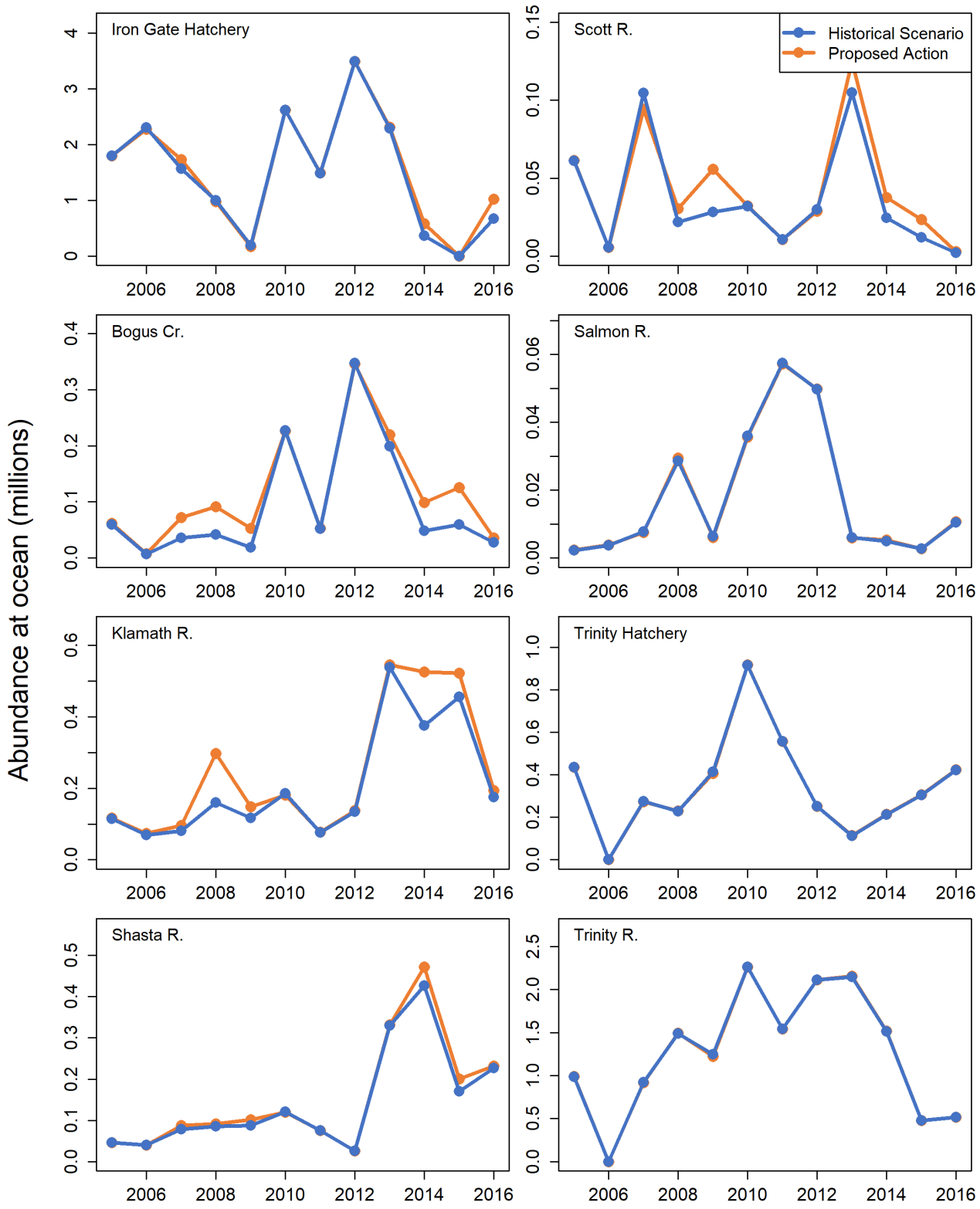

Figure 17. Graphs showing annual juvenile fall Chinook salmon abundances—simulated by the Stream Salmonid Simulator model under the Historical and Proposed Action scenarios—at the Pacific Ocean, California, 2005–16. Cr., Creek; R., River.

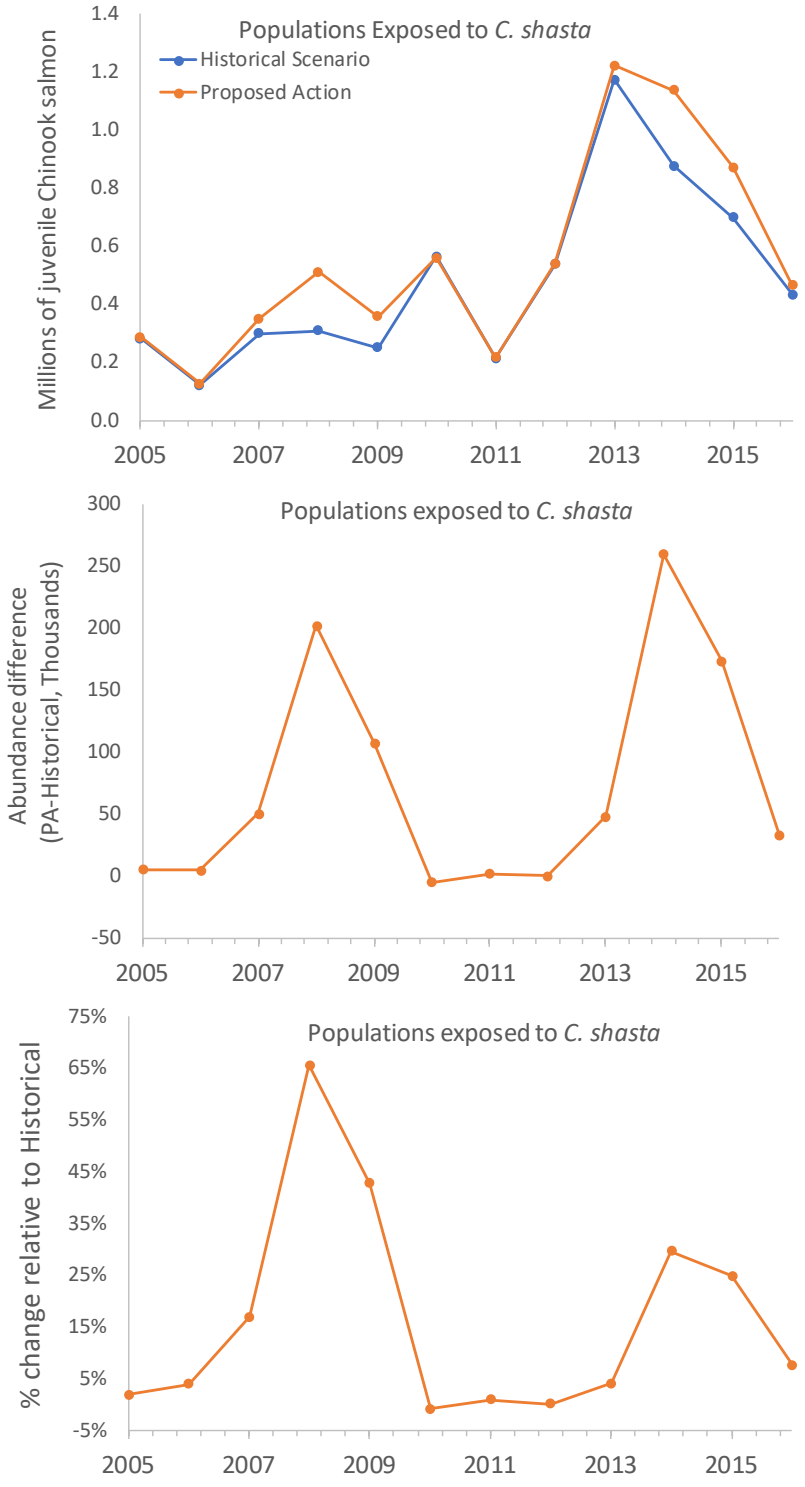

Figure 18. Graphs showing annual abundance, the difference in abundance, and the percent (%) change in abundance for simulated juvenile fall Chinook salmon at the Pacific Ocean simulated by the Stream Salmonid Simulator model for the combined tributary source populations exposed to the disease zone—Klamath River, Bogus Creek Scott River, and Shasta River, Klamath River Basin, California, 2005–16. *C. shasta*, *Ceratonova shasta*; PA, Proposed Action.

Adult Equivalent Returns

Calculation of age-4 adult equivalents represents juvenile salmon abundance at ocean entry while accounting for the average age-specific survival through age 4 in the ocean. The number of age-4 adult equivalents was of similar magnitude to the observed returns of spawning adults to the main-stem Klamath River (table 7). For example, the observed return of spawning females to the main-stem Klamath River ranged from 1,947 to 10,624 (table 1) and estimates of the adult equivalents to the main-stem Klamath River ranged from 927 to 7,174 under the HI scenario and from 984 to 7,253 under the PA scenario. The total number of adult equivalents from all tributary sources ranged from 19,701 to 85,759 under the HI scenario and ranged from 22,036 to 85,745 adult equivalents under the PA scenario.

Table 7. Annual adult equivalents based on applying ocean survival rates in Hankin and Logan (2010) to juvenile salmon abundance at ocean entry simulated by the Stream Salmonid Simulator model, Klamath River Basin, California, 2005–16.

[Estimates are shown by tributary and hatchery sources of juvenile fish to the Klamath River under the Historical and Proposed Action scenarios. Because of high flows, estimates of Trinity River fish entering the Klamath River were not available during 2006 (as indicated by symbol –)]

Migration year	Klamath River	Klamath hatchery	Bogus Creek	Salmon River	Scott River	Shasta River	Trinity hatchery	Trinity River	Annual total
					Historical				
2005	1,530	23,961	792	30	812	608	5,798	13,110	46,641
2006	927	30,625	93	50	74	534	–	–	32,303
2007	1,070	20,823	476	104	1,391	1,048	3,667	12,277	40,855
2008	2,133	13,244	550	381	289	1,133	3,044	19,837	40,612
2009	1,550	2,597	251	85	376	1,163	5,505	16,580	28,106
2010	2,463	34,873	3,023	478	427	1,607	12,188	30,124	85,183
2011	1,009	19,745	694	764	143	997	7,419	20,530	51,301
2012	1,796	46,459	4,621	662	396	349	3,340	28,136	85,759
2013	7,174	30,496	2,650	80	1,396	4,390	1,485	28,562	76,233
2014	4,997	4,862	641	65	325	5,681	2,828	20,152	39,551
2015	6,073	1	791	35	159	2,261	4,061	6,321	19,701
2016	2,337	8,917	369	139	26	3,015	5,601	6,849	27,254
					Proposed Action				
2005	1,558	23,963	824	31	818	613	5,805	13,159	46,771
2006	984	30,286	102	51	74	533	–	–	32,031
2007	1,280	23,004	962	100	1,254	1,163	3,644	12,239	43,645
2008	3,953	13,008	1,219	391	406	1,220	3,048	19,877	43,122
2009	1,968	2,285	705	80	742	1,352	5,409	16,252	28,793
2010	2,416	34,884	3,017	474	430	1,592	12,190	30,109	85,113
2011	1,026	19,844	701	761	142	1,001	7,406	20,495	51,377
2012	1,834	46,437	4,603	664	381	350	3,335	28,141	85,745
2013	7,253	30,788	2,928	79	1,662	4,407	1,515	28,689	77,320
2014	7,001	7,714	1,313	70	499	6,283	2,847	20,175	45,902
2015	6,951	1	1,669	36	313	2,662	4,084	6,321	22,036
2016	2,586	13,568	477	142	40	3,084	5,643	6,879	32,419

Discussion

This document presents the first use of the S3 model to help inform management actions relevant to the operation of dams on the lower Klamath River. In this application, we focused on the hypothesized effects of management actions intended to lessen the prevalence of infection and mortality of juvenile Chinook salmon caused by the myxozoan parasite *C. shasta*. The S3 model provides a unique mesoscale perspective on the population dynamics of juvenile fall Chinook salmon by modelling the spatiotemporal dynamics of juvenile salmon growth, movement, and survival in response to river flow, habitat availability, and water temperature at daily time scales important to Iron Gate Dam operations. These attributes make the S3 model a powerful tool for exploring how management actions that alter daily flow and water temperature of the Klamath River also influence spore concentration and juvenile salmon population dynamics.

The HI scenario was based on the historical record of flows, temperatures, and spore concentrations, whereas the PA scenario included a relatively high frequency of surface flushing flows early in the juvenile salmon migration season that are anticipated to decrease *C. shasta* spore concentrations and juvenile salmon mortality risk during out-migration. The PA scenario targeted at least 3 consecutive days of river flow no less than 6,030 ft^3/s. Given that the S3 model incorporated the same physical and biological inputs among the scenarios (except flow, water temperature, and spore concentrations), model outputs represent these key differences between the scenarios.

We used two key locations to summarize S3 model output under each scenario because output at each location provides different insights and inferences about mortality and disease. First, although the *C. shasta* infectious zone extends downstream of the Kinsman Creek trap site, juvenile fish monitoring data at this location provides critical information to fishery and water managers about annual abundance, migration timing, and *C. shasta* disease incidence. Managers have come to understand the scale and magnitude of disease prevalence based the empirical population estimates passing Kinsman Creek Thus, model output at Kinsman Creek can be judged directly in the context of empirical data at this location. However, the drawback of using model output at only this site is that mortality due to disease manifests well downstream of the infectious zone, as our simulation results indicate. Therefore, the ocean also is a key location for model output because (1) survival to ocean entry encapsulates the total in-river mortality and differences between scenarios, and (2) it measures the population size at the ecotone between freshwater and ocean environments.

At the Kinsman Creek trap site, fish abundance was only slightly higher under the PA scenario compared to the HI scenario, but the prevalence of infection was markedly lower for simulated fish migrating under the PA scenario compared to the HI scenario. The effect of the PA scenario on infection and mortality by *C. shasta* varied among years in response to the seasonal spore concentration regime of each year. In years when spore concentrations were relatively low, the PA scenario provided little benefit over the HI scenario, but when spore concentrations were relatively high, the PA scenario decreased *C. shasta* infection rates at the Kinsman Creek trap site and increased juvenile salmon survival to the ocean. Survival of fish to the Kinsman Creek trap site was nearly identical between the HI and PA scenarios, which be expected given that *C. shasta* mortality is time-dependent and that mortality is unlikely to manifest at this upriver location early in migration season.

In contrast, the simulated outcomes at the Pacific Ocean fully indicated the consequence of *C. shasta* exposure for different source populations and scenarios. Under the PA scenario, the S3 model indicated modest increases in abundance at ocean entry. For natural populations only exposed to the diseases zone (that is, Bogus Creek, and Klamath, Scott, and Shasta Rivers), the PA scenario increased fish abundance at ocean entry over the HI scenario (PA - HI) by as much as 210,233 fish in migration year 2014, but as few as 37 fish in migration year 2011.

In addition to differences in survival to the ocean, our model indicated many infected juvenile salmon survived to ocean entry under both scenarios. As described in section, "Methods," infected fish in our model are those that are expected to die from disease at some future date. Whether fish die in-river or survive to ocean entry is dictated by migration rate (a function of fish density and fish size) and the rate per unit time at which infected fish die (a function of spore concentration during exposure, exposure duration, and water temperature). Although the true fate of infected fish that survive to the ocean is unknown, it is critical to emphasize that these fish would have been expected to die based on our analysis of sentinel experiment data where the time to death is measured for as many as 90 days post-exposure (Ray and others, 2014; Perry and others, 2019). Thus, when the goal of management actions is to decrease disease impacts, managers should consider differences in in-river mortality and simulated prevalence of infection to gauge the effects of different scenarios on juvenile salmon populations.

Perhaps the most counter-intuitive result was the simulated higher prevalence of infection at ocean entry under the PA scenario—particularly for Klamath River and Bogus Creek juvenile salmon. The lower prevalence of infection by *C. shasta* at ocean entry under the HI scenario was driven by higher in-river mortality of infected fish relative to the PA scenario. Thus, more infected fish were removed from the population prior to ocean entry under the HI scenario, driving down the prevalence of infection at ocean entry. In contrast, under the PA scenario, lower spore concentrations not only decrease the prevalence of infection but also increase the time to death, thereby increasing the number of infected fish surviving to ocean entry.

Our model also shows how differential time-dependent mortality among years could affect inferences about the prevalence of infection from empirical estimates at the Kinsman Creek trap. For example, considerably higher spore concentrations occurred in 2015 than in all other years (fig. 3) yet the simulated prevalence of infection at the Kinsman Trap was only the fifth highest under the HI scenario. Spore concentrations were so high, however, that the time to death of infected fish was decreased enough to increase *C. shasta*-caused mortality upstream of the Kinsman Creek Trap (fig. 8), thereby removing infected fish from the population and reducing the apparent prevalence of infection at Kinsman Creek

Our simulations showed how the timing of flushing flows can substantially affect the degree to which management actions decrease disease. We hypothesized that annual flushing flows greater than 6,030 ft^3/s for 3 or more days would delay the onset of increasing spore concentrations and decrease spore concentrations proportionally to the decrease in polychaete habitat area. The largest difference in the prevalence of infection at the Kinsman Creek trap site between the scenarios occurred in 2014 (fig. 11), when mid-April flushing flows kept spore concentrations low until early May (fig. 2), which allowed much of the juvenile salmon population to pass through the infectious zone before spore concentrations increased (fig. 3). Although spore concentrations decreased in all years in response to Proposed Action flushing flows, in only 2005, 2006, and 2014 did flushing flows occur late enough in the year to delay the onset of increasing spore concentrations. Thus, our simulation was able to show how different aspects of management actions affect disease outcomes.

By using estimates of age-specific survival for Iron Gate Hatchery fish from Hankin and Logan (2010), we calculated the adult (age-4) equivalents that might survive to return to the Klamath River for each tributary source population. For populations exposed to the disease zone (that is, Bogus Creek, and Klamath, Shasta, and Scott Rivers) there was, on average, 978 more adult equivalents (PA-HI) under the PA scenario than under the HI scenario. Thus, the relative changes in flow under the PA scenario resulted in a noticeable, but modest increase in the number of adults that may return from a given annual cohort of juvenile salmon. Estimates of the adult equivalents from the S3 model simulations were similar in magnitude (thousands) to those that have been measured historically within the Klamath River, suggesting that the S3 model output was providing reasonably good estimates of production for the Klamath River and its tributary sources.

The S3 model provides a powerful tool for objectively comparing flow, temperature, and disease management questions about juvenile salmon by incorporating the best available science about specific life stages for Klamath River Chinook salmon, such as (1) spawning and fecundity; (2) water temperature, egg maturation, and fry emergence; (3) abundance and entry timing of tributary source populations; (4) habitat availability in relation to juvenile fish growth, movement, and survival during freshwater rearing; and (5) the spatial extent and exposure of fish to *C. shasta.*. We used the S3 model to compare a set of flows and spore-concentration scenarios, and inputs such as the abundances of spawning females and juveniles entering from tributaries and hatcheries and water temperatures held constant among scenarios. In contrast, flows and spore concentrations differed between the PA and HI scenarios. Incorporating the daily similarities and differences among the scenarios enabled an objective comparison between the scenario outcomes. The S3 model provides a mesoscale view of fish growth, survival, and migration from spawning to ocean entry, and model output can be summarized at daily and habitat-unit scales, providing information about the abundance, survival, and disease exposures for juvenile salmon under a particular set of prespecified conditions. These attributes make the S3 model unique and enable the objective assessment of questions about flow and disease management in the Klamath River that could not otherwise be obtained.

Acknowledgments

We are grateful to staff of multiple State, Federal, and Tribal agencies who have collected the field data on which our modeling efforts are based, and to a broad coalition of Federal and State agency, Tribal, and university scientists that contributed to the development of the S3 model through their participation in technical workshops.

References Cited

Bartholomew, J., Hallett, S., Holt, R., , Alexander, J., Buckles, G., Ray, A., Craig, R., and Atkinson, S., 2015, Klamath River fish health studies—Second reporting cycle, April 01, 2014–June 30, 2015—Annual report: Salem, Oregon State University, GSA Contract GS09T13BHD0052, 49 p.

Bureau of Reclamation, 2018, Bureau of Reclamation hydrologic assessment relative to court injunction: United States District Court for Northern District of California, San Francisco Division, Case 3:16-cv-04294-WHO Document 144-2, filed March 3, 2018.

Bureau of Reclamation, 2019, Addendum to the Proposed Action included in Reclamation's 2018 final biological assessment on the effects of the Proposed Action to operate the Klamath Project on federally-listed threatened and endangered species. Document emailed to the National Marine Fisheries Service by the Bureau of Reclamation on February 15, 2019, https://www.usbr.gov/mp/kbao/docs/final-2018-ba-klamath-project-ops.pdf.

California Rivers Assessment, 2011, Watershed information by basin, average precipitation per year: California Rivers Assessment, Watershed database, accessed November 13, 2018, at http://ice.ucdavis.edu/project/cara.

Daniels, S.S., Debrick, A., Diviney, C., Underwood, K., Stenhouse, S., and Chesney, W.R., 2011, Final report—Shasta and Scott River juvenile outmigrant study, 2010: California Department of Fish and Game, Report Number P0710307, 97 p.

Gough, S.A., David, A.T., and Pinnix, W.D., 2015, Summary of abundance and biological data collected during juvenile salmonid monitoring in the mainstem Klamath River below Iron Gate Dam, California, 2000–2013: Arcata, California, U.S. Fish and Wildlife Service, Arcata Fish and Wildlife Office, Arcata Fisheries Data Series Report Number DS 2015-43, 95 p. plus appendixes.

Gough, S.A., and Som, N.S., 2015, Fall Chinook salmon run characteristics and escapement for the mainstem Klamath River, 2013–2015: Arcata, California, U.S. Fish and Wildlife Service, Arcata Fish and Wildlife Office, Arcata Fisheries Data Series Report Number DS 2017-50, 34 p.

Hallett, S.L., and Bartholomew, J.L., 2006, Application of real-time PCR assay to detect and quantify the myxozoan parasite *Ceratomyxa shasta* in river water samples: Diseases of Aquatic Organisms, v. 71, p. 109–118.

Hankin, D.G., and Logan, E., 2010, A preliminary analysis of Chinook salmon coded-wire tag recovery data from Iron Gate, Trinity River and Cole Rivers Hatcheries, brood years 1978–2004: Prepared for The Hoopa Valley Tribal Council and the Arcata Office, U.S. Fish and Wildlife Service, 65 p. [Also available at https://www.fws.gov/arcata/fisheries/reports/technical/IGHTRH.CWTanalysis2009%20Hankin%20Rpt.pdf.]

Hardy, T.B., and Shaw, T., 2011, SALMOD—Meso-habitat development Keno to estuary, *in* Hendrix, N., Campbell, S., Hampton, M., Hardy, T., Huntington, C., Lindley, S., Perry, R., Shaw, T., and Williamson, S., Fall Chinook salmon life cycle production model report to expert panel: Prepared for Expert Panel reviewing Chinook salmon of the Klamath River Basin, p. 4-1–4-32, accessed March 26, 2019, at https://www.fws.gov/arcata/fisheries/reports/technical/Fall%20Chinook%20Report%20of%20FPM%20Team%20to%20Expert%20Panel%20DRAFT%201%202011.pdf.

National Marine Fisheries Service, 2019, Endangered Species Act Section 7(a)(2) biological opinion, and Magnuson-Stevens Fishery Conservation and Management Act essential fish habitat response for Klamath Project Operations from April 1, 2019 through March 31, 2024: Letter to Jeffrey Nettleton, Area Manager, Klamath Basin Area Office Bureau of Reclamation, https://www.westcoast.fisheries.noaa.gov/publications/Klamath/19-03-29_nmfs_biop_klamath_project_operations.pdf.

Perry, R.W., Plumb, J.M., Jones, E.C., Som, N.A., Hardy, T.B., and Hetrick, N.J., 2019, Application of the Stream Salmonid Simulator (S3) to Klamath River fall Chinook salmon (*Oncorhynchus tshawytscha*), California—Parameterization and calibration: U.S. Geological Survey Open-File Report 2019–1107, 89 p., https://doi.org/10.3133/ofr20191107.

Perry, R.W., Plumb, J.M., Jones, E.C., Som, N.A., Hetrick, N.J., and Hardy, T.B., 2018, Model structure of the stream salmonid simulator (S3)—A dynamic model for simulating growth, movement, and survival of juvenile salmonids: U.S. Geological Survey Open-File Report 2018-1056.

Perry, R.W., Risley, J.C., Brewer, S.J., Jones, E.C., and Rondorf, D.W., 2011, Simulating daily water temperatures of the Klamath River under dam removal and climate change scenarios: U.S. Geological Survey Open-File Report 2011-1243, 78 p.

Ray, R.A., Perry, R.W., Som, N.A., and Bartholomew, J.L., 2014, Using cure models for analyzing the influence of pathogens on salmon survival: Transactions of the American Fisheries Society, v. 143, p. 387–398.

Rymer, R., 2008, Reuniting a river—Klamath Forest Alliance: Klamath Forest Alliance web page, accessed November 13, 2018, at http://www.klamathforestalliance.org/Newsarticles/newsarticle20081201.html.

Som, N.A., Hetrick, N.J., Alexander, J., Shea, C., Foott, J.S., and True, K., 2016, Technical memorandums regarding *Ceratonova shasta* in the Klamath River—Response to request for technical assistance from the Yurok and Karuk Tribes: Arcata, California, U.S. Fish and Wildlife Service, Arcata Fish and Wildlife Office, https://www.fws.gov/arcata/fisheries/reportsDisplay.html.

U.S. Department of Interior, 2013, Klamath Dam removal overview report for the Secretary of the Interior—An assessment of science and technical information: Prepared by U.S. Department of Interior and U.S. Department of Commerce, National Marine Fisheries Service, 420 p., accessed November 13, 2018, at https://klamathrestoration.gov/sites/klamathrestoration.gov/files/Full%20SDOR%20accessible%20022216.pdf.

Weddell, B.J., 2000, Relationship between flows in the Klamath River and Lower Klamath Lake prior to 1910: U. S. Department of Interior Fish and Wildlife Service Klamath Basin Refuges, Tulelake, California, 15 p.

Publishing support provided by the U.S. Geological Survey
Science Publishing Network, Tacoma Publishing Service Center

For more information concerning the research in this report, contact the
Director, Western Fisheries Research Center
U.S. Geological Survey
6505 NE 65th Street
Seattle, Washington 98115-5016
https://www.usgs.gov/centers/wfrc

ISSN 2331-1258 (online)
https://doi.org/10.3133/ofr20191099